Snaking of localized time-dependent oscillations

Edgar Knobloch

Department of Physics
University of California, Berkeley, CA 94720, USA

knobloch@berkeley.edu

Joint work with Hannes Uecker, Nicolas Verschueren,
Saar Modai and Arik Yochelis

ICERM, Providence, 27 April 2026

Wall and bulk modes in the Swift-Hohenberg equation

The Swift-Hohenberg equation RSHE35 on a disk

$$\partial_t u = \epsilon u + \nu u^3 - u^5 - (q^2 + \Delta)^2 u,$$

with $\nabla u \cdot \hat{n}|_{\partial\Omega} = 0$, $\nabla(\Delta u) \cdot \hat{n}|_{\partial\Omega} = 0$ is a gradient system on Ω and hence possesses only steady states as $t \to \infty$:

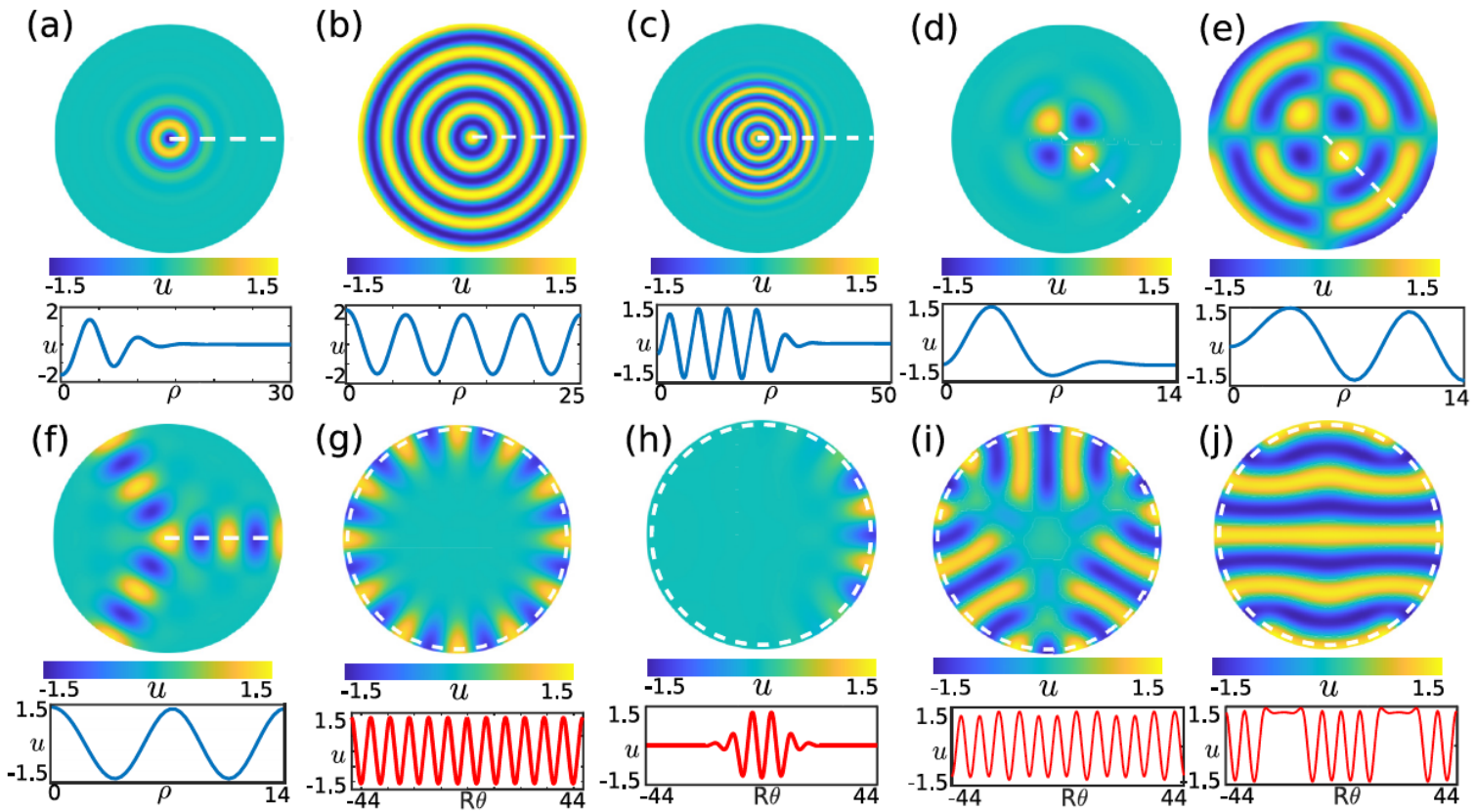

RSHE35: Eigenfunctions of the $u = 0$ solution

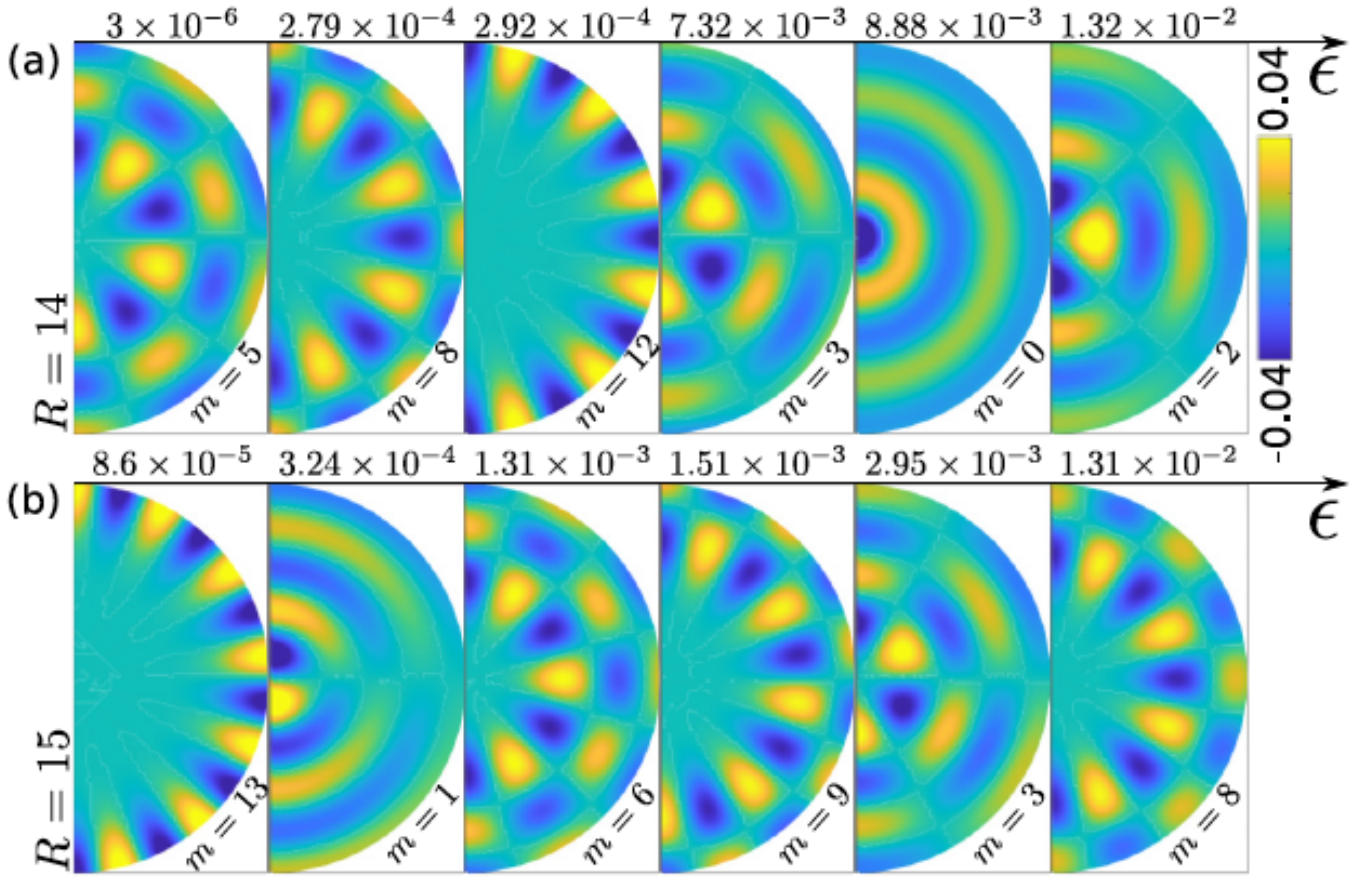

FIG. 3. The first six eigenfunctions on the half disk predicted by linear stability analysis of the $u = 0$ state when (a) $R = 14$ and (b) $R = 15$. The eigenfunctions are sorted according to the eigenvalues ε. In each case, ε and the corresponding azimuthal number m are specified.

RSHE35: Wall and bulk modes with symmetry D_m

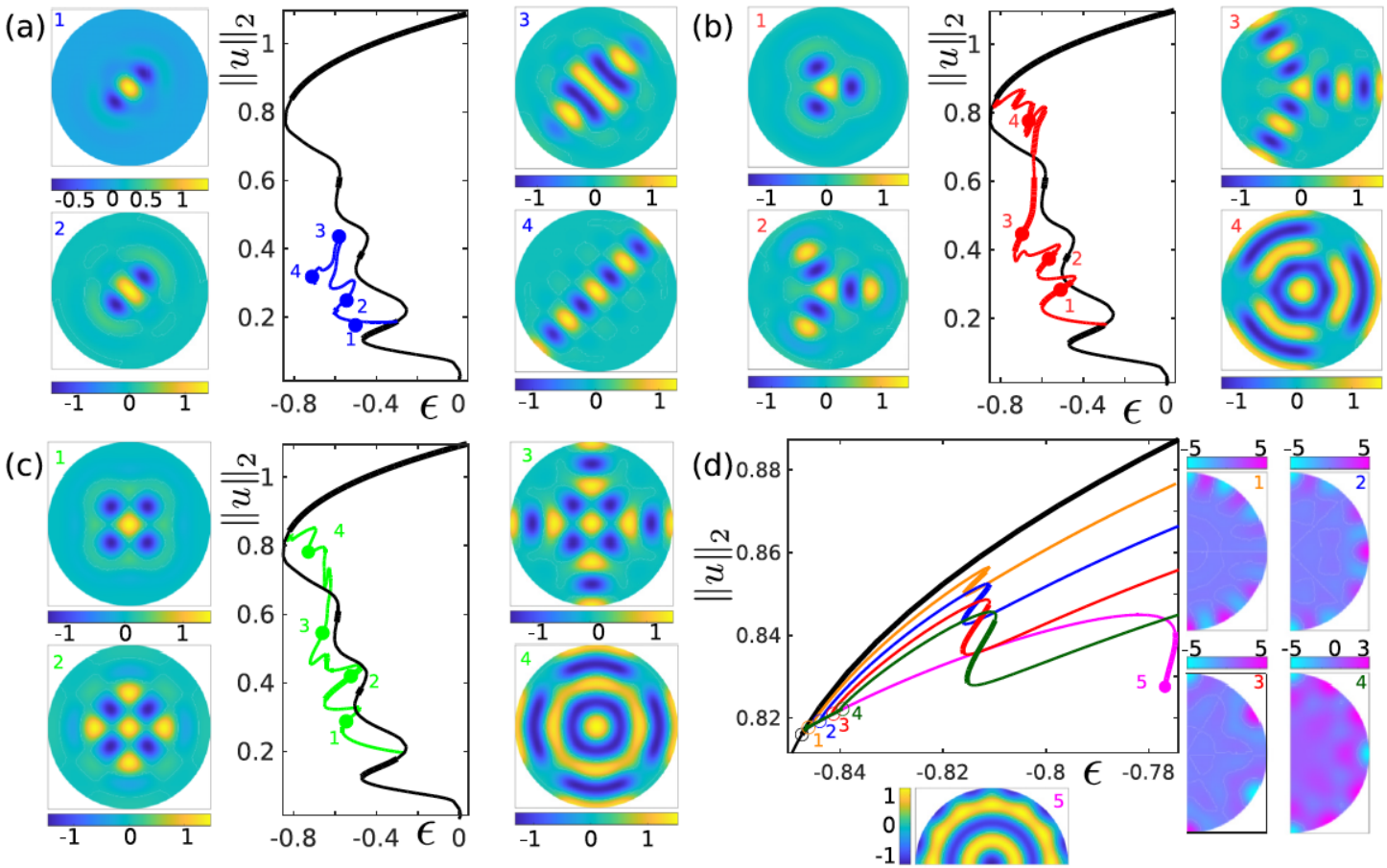

Verschueren et al., PRE **104**, 014208 (2021)

RSHE35: Wall and bulk modes with symmetry D_m^-

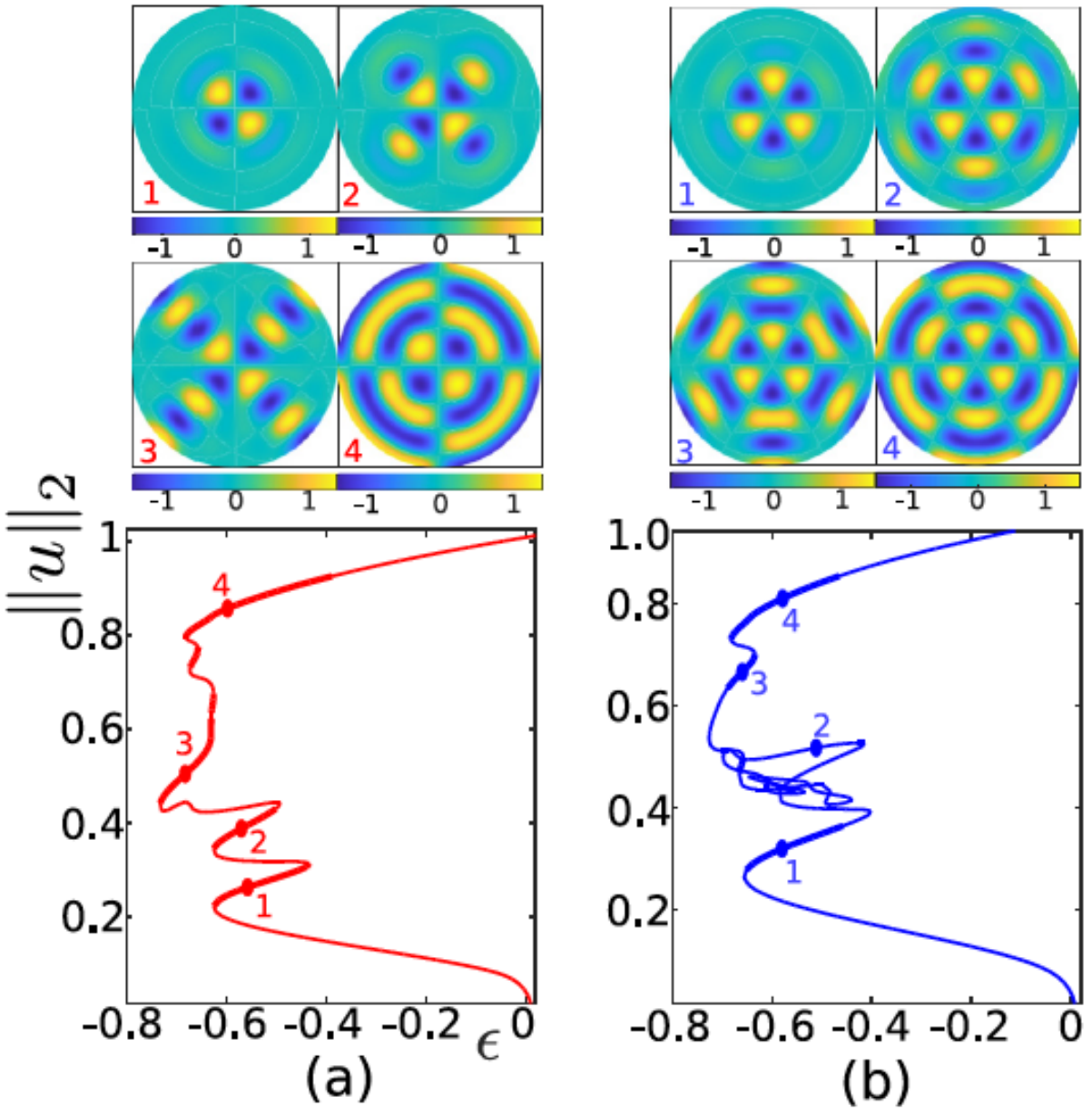

RSHE35: Wall modes and homoclinic snaking

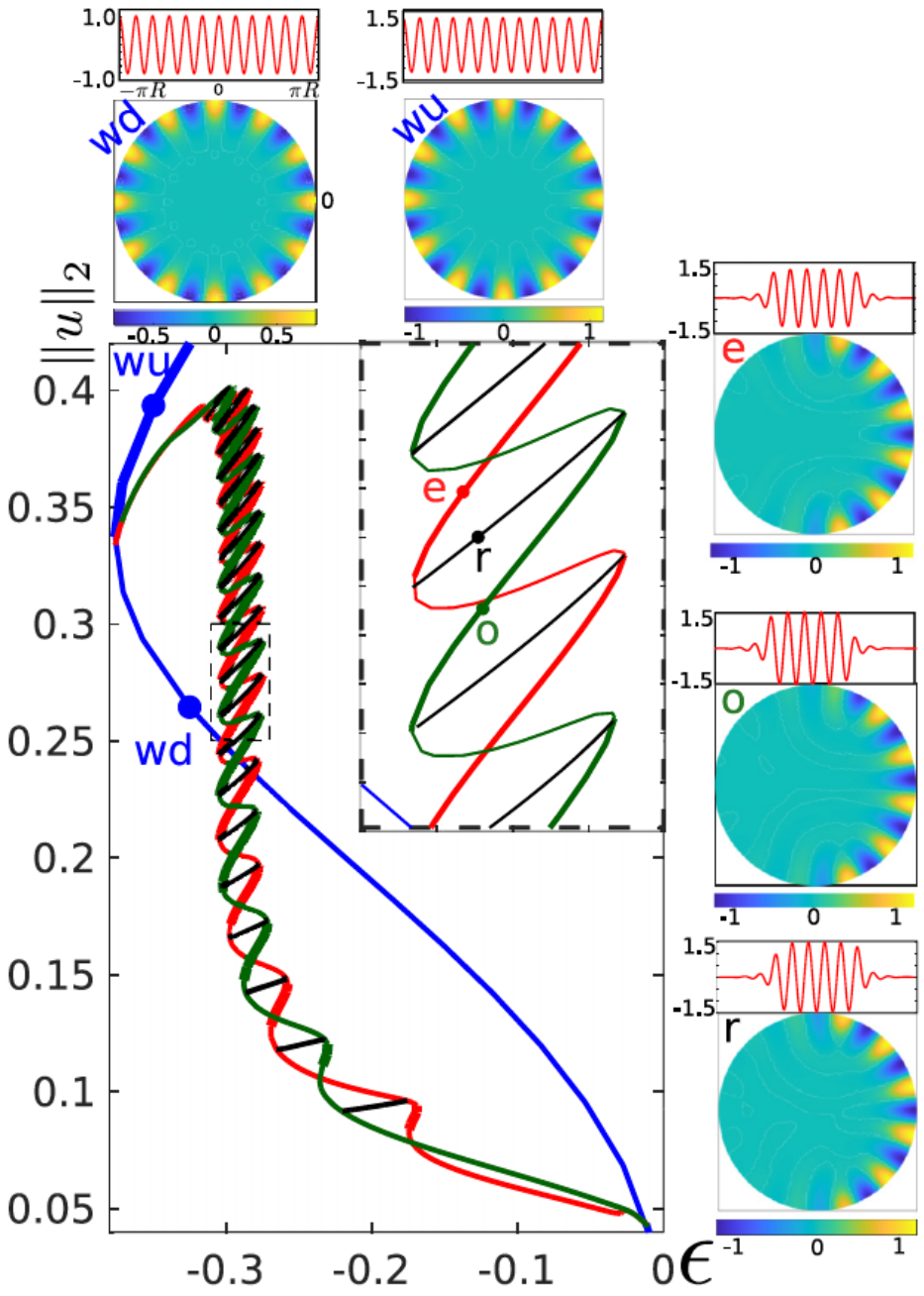

Burke and Knobloch, Chaos **17**, 037102 (2007)

Beck et al., SIAM J. Math. Anal. **41**, 936 (2009)

Verschueren et al., PRE **104**, 014208 (2021)

Complex Swift-Hohenberg equation in 1D and 2D

The complex Swift-Hohenberg equation CSHE35

$$\partial_t u = (\lambda + i\nu)u - (c_3 + i\gamma)|u|^2 u - |u|^4 u - (1+\Delta)^2 u + i\delta\Delta u,$$

with $u = u(x,t) \in \mathcal{C}$ and coefficients $\lambda, \nu, \delta, c_3, \gamma \in \mathcal{R}$, is not a gradient system and so admits oscillations. We consider two cases

$$\Omega_1 = [-\ell/2, \ell/2), \qquad \Omega_2 = \{\mathbf{x}{=}r(\cos\vartheta, \sin\vartheta) : r{\in}[0,R], \vartheta{\in}[-\pi,\pi)\}.$$

with periodic boundary conditions (pBCs) on Ω_1

$$\partial_x^j u(-\ell/2) = \partial_x^j u(\ell/2), \quad j = 0, \ldots, 3$$

for a domain of length ℓ, and Neumann boundary conditions (NBCs)

$$\nabla u \cdot \hat{n}|_{\partial\Omega_2} = 0, \qquad \nabla(\Delta u) \cdot \hat{n}|_{\partial\Omega_2} = 0$$

on Ω_2. Here $\hat{n}$ represents the outward unit normal.

The equation is solved using pde2path written by Hannes Uecker.

Complex Swift-Hohenberg equation in 1D and 2D

We are interested in the following solution types:

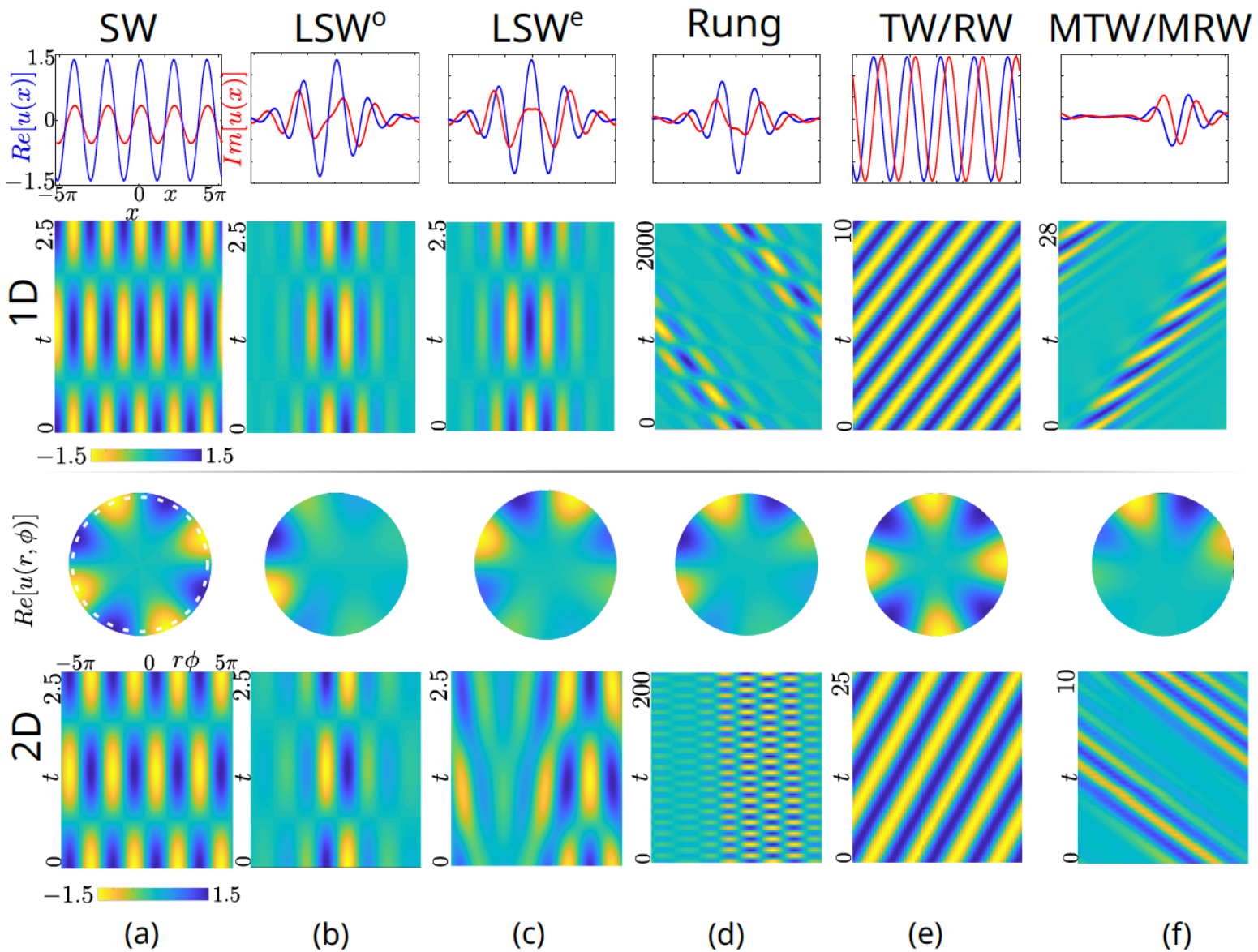

Complex Swift-Hohenberg equation in 1D and 2D

TABLE I. Solution classes,symmetries, and acronyms; in 2D (second block) we use (r, ϑ) for the polar coordinates on the disk.

Type	**order**	**origin, form and symmetries**
TW	prim.	traveling wave, bifurcating from $u \equiv 0$, $u_{\mathrm{TW}}(x,t) = \alpha e^{\mathrm{i}(kx-\omega_{\mathrm{TW}}t)}$, see (5); $\lvert u\rvert$ constant in space and time, relative equilibrium in comoving frame with speed $s = \omega_{\mathrm{TW}}/k$.
SW	prim.	standing wave, bifurcating from $u \equiv 0$, $u_{\mathrm{SW}}(x,t) = v(x)e^{-\mathrm{i}\omega_{\mathrm{SW}}t}$, see (34); $\lvert u\rvert$ constant in time, relative equilibrium in gauge rotating frame.
MTW	second.	modulated TW, bifurcating from TWs, $u_{\mathrm{MTW}}(x,t)=v(x-s_2t)e^{\mathrm{i}(kx-\omega t)}$, see (37), but (numerically) computed as relative PO in frame with (average) speed s; $\lvert u\rvert$ constant in time in frame moving with speed s_2, with $s_2 = \mathcal{O}(1)$ in general, in particular at onset.
LSW	second.	localized standing wave, bifurcating from SWs, same form as SW, with spatially localized v.
LDW	tert.	localized drifting wave, $u_{\mathrm{LDW}}(x,t) = v(x-st)e^{-\mathrm{i}\omega t}$, bifurcating from LSWs in a drift bifurcation, i.e., with speed $s = 0$ at onset; relative equilibrium in comoving and gauge rotating frame.
2-freq.LSW	tert.	two-frequency LSW, bifurcating from LSWs, $u(x,t) = v(x,t)e^{-\mathrm{i}\omega t}$ with v periodic in time with period $T > 0$, $\lvert u\rvert$ not constant in space or time. Similarly for 2-freq. SWs, which bifurcate from SWs.
RW	prim.	rotating wave, bifurcating from $u \equiv 0$, $u_{\mathrm{RW}}(x,t) = v(r)e^{\mathrm{i}(m\vartheta-\omega_{\mathrm{RW}}t)}$, see (9); $\lvert u\rvert$ constant in ϑ, t, relative equilibrium in corotating frame with speed $s = \omega_{\mathrm{RW}}/m$.
SW	prim.	standing wave, bifurcating from $u\equiv 0$, like 1D (dimension-indep.), $u_{\mathrm{SW}}(x,t)=v(x)e^{-\mathrm{i}\omega_{\mathrm{SW}}t}$, see (34).
MRW	second.	modulated RW, bifurcating from RWs, $u_{\mathrm{MRW}}(x,t) = v(r,\vartheta - s_2t))e^{\mathrm{i}(m\vartheta-\omega_{\mathrm{RW}}t)}$, but (numerically) computed as relative PO in frame rotating with (average) speed s; $\lvert u\rvert$ constant in time in frame rotating with speed s_2.
LSW	second.	localized SW, bifurcating from SWs, with $v(x)$ localized in angle ϑ.
LDW	tert.	as in 1D, bifurcating from LSWs, with drift in ϑ.
2-freq.LSW	tert.	two-frequency LSW, as in 1D, bifurcating from LSWs.

Uecker et al., preprint

Complex Swift-Hohenberg equation in 1D: MTW

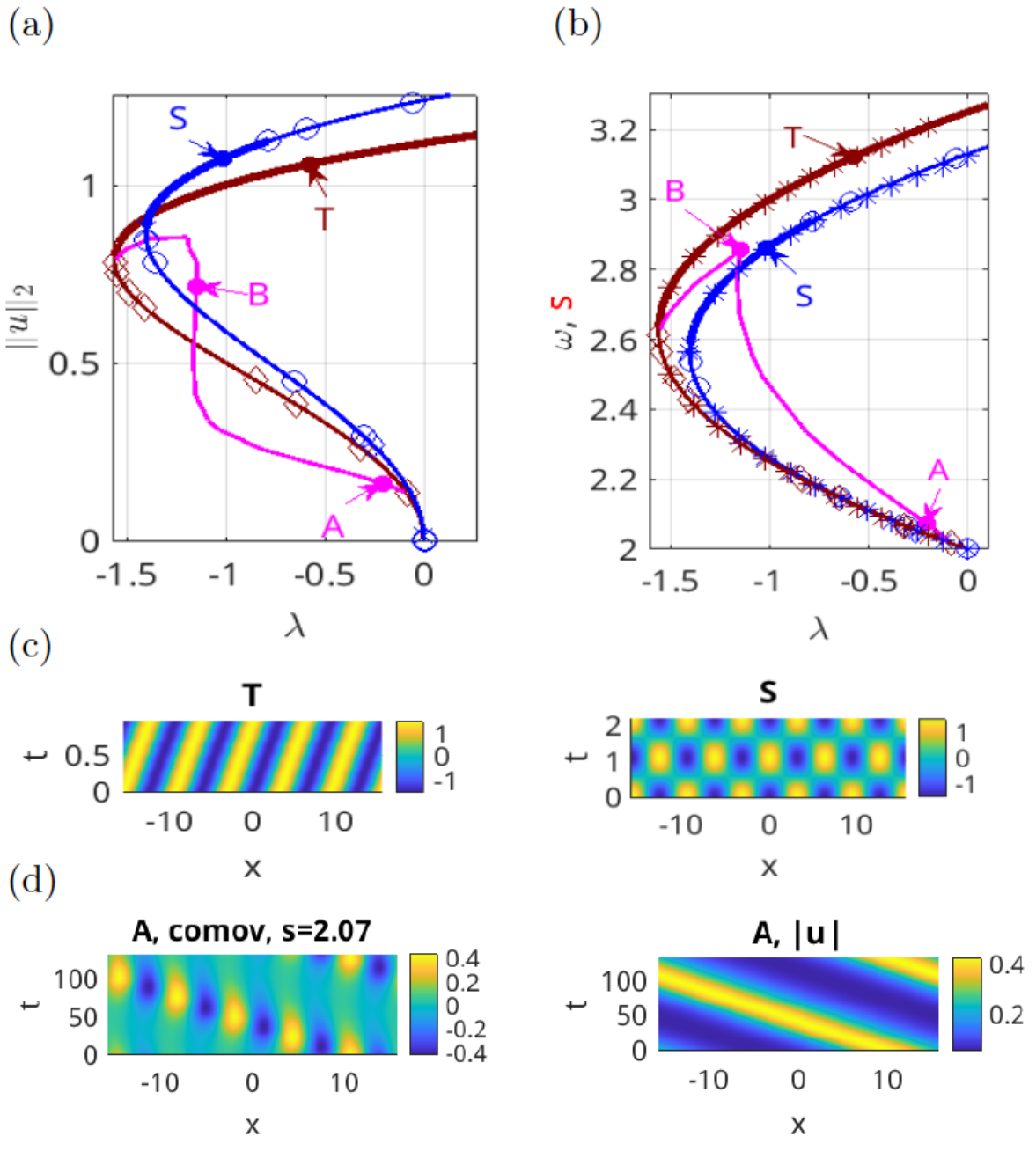

Complex Swift-Hohenberg equation in 1D: LSW

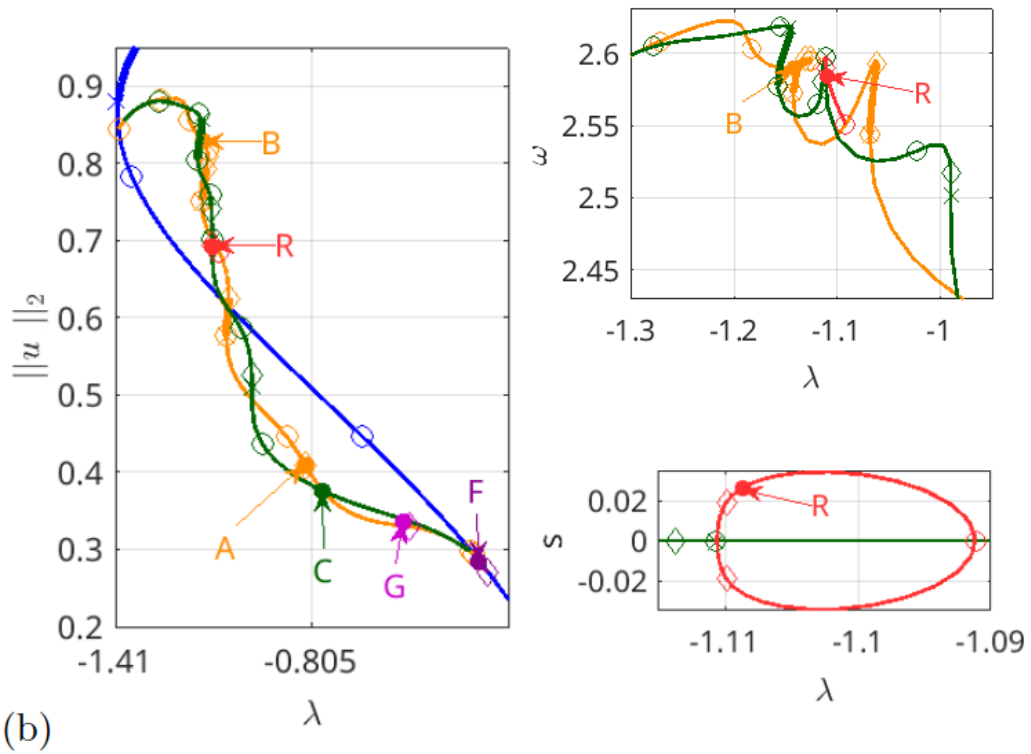

(b)

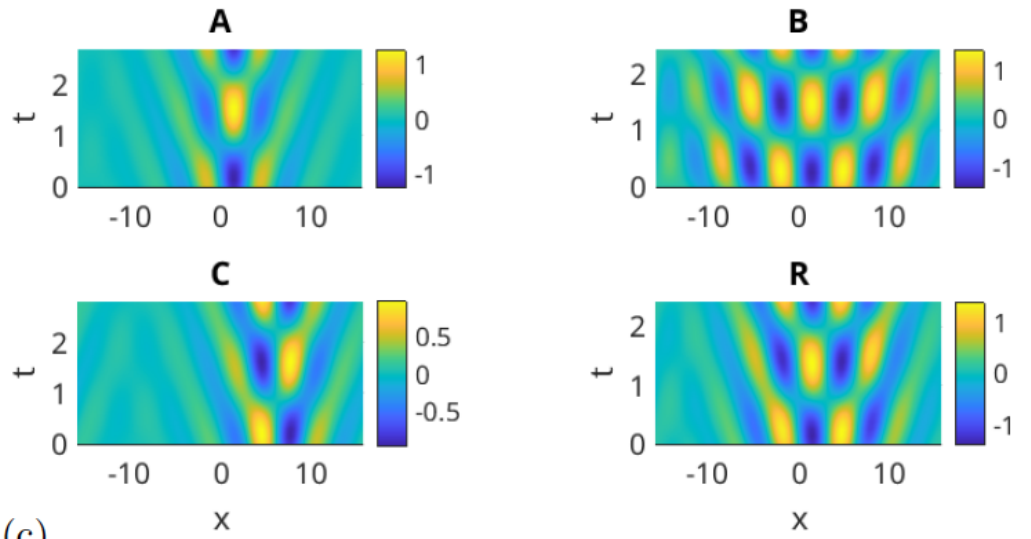

(c)

CSHE35: LSW and MTW

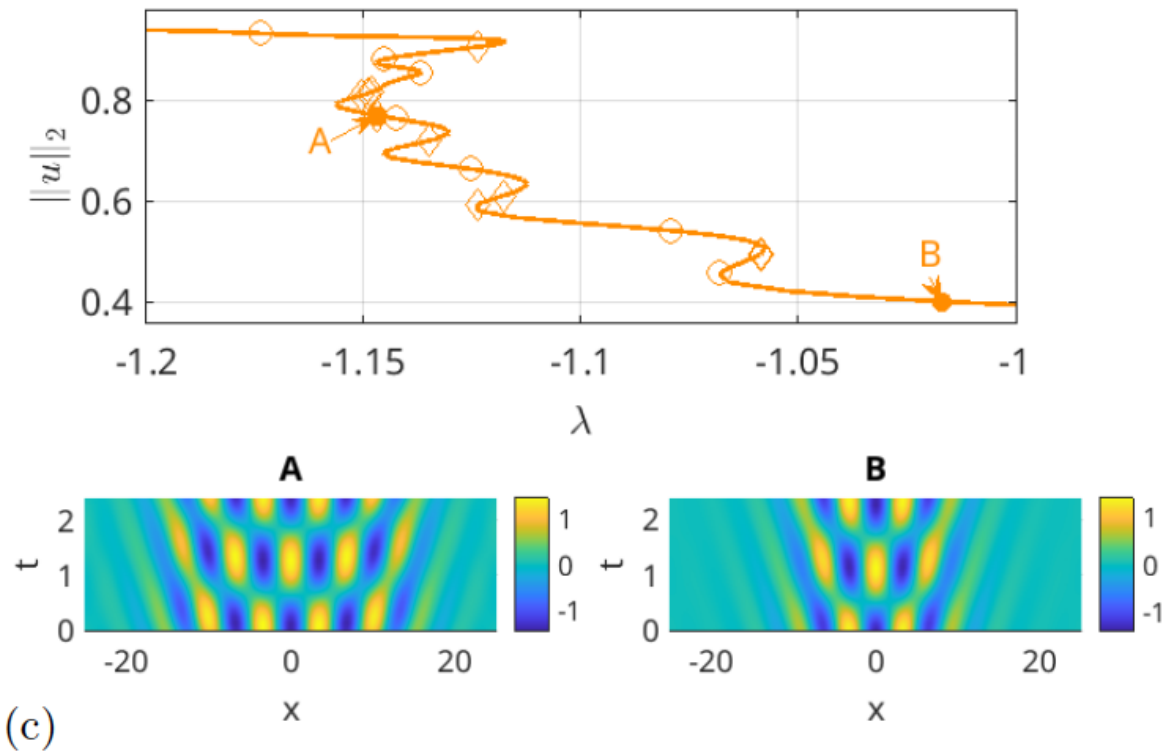

(c)

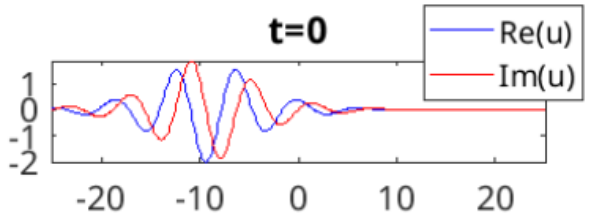

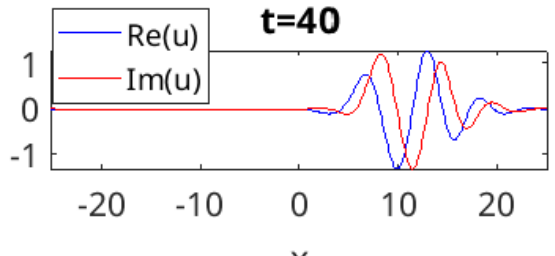

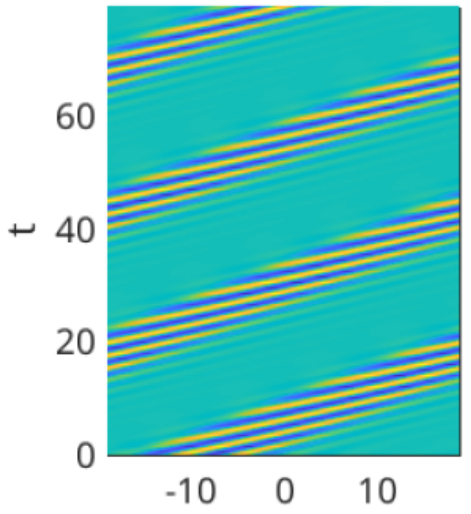

CSHE35: LSWs and DLSW

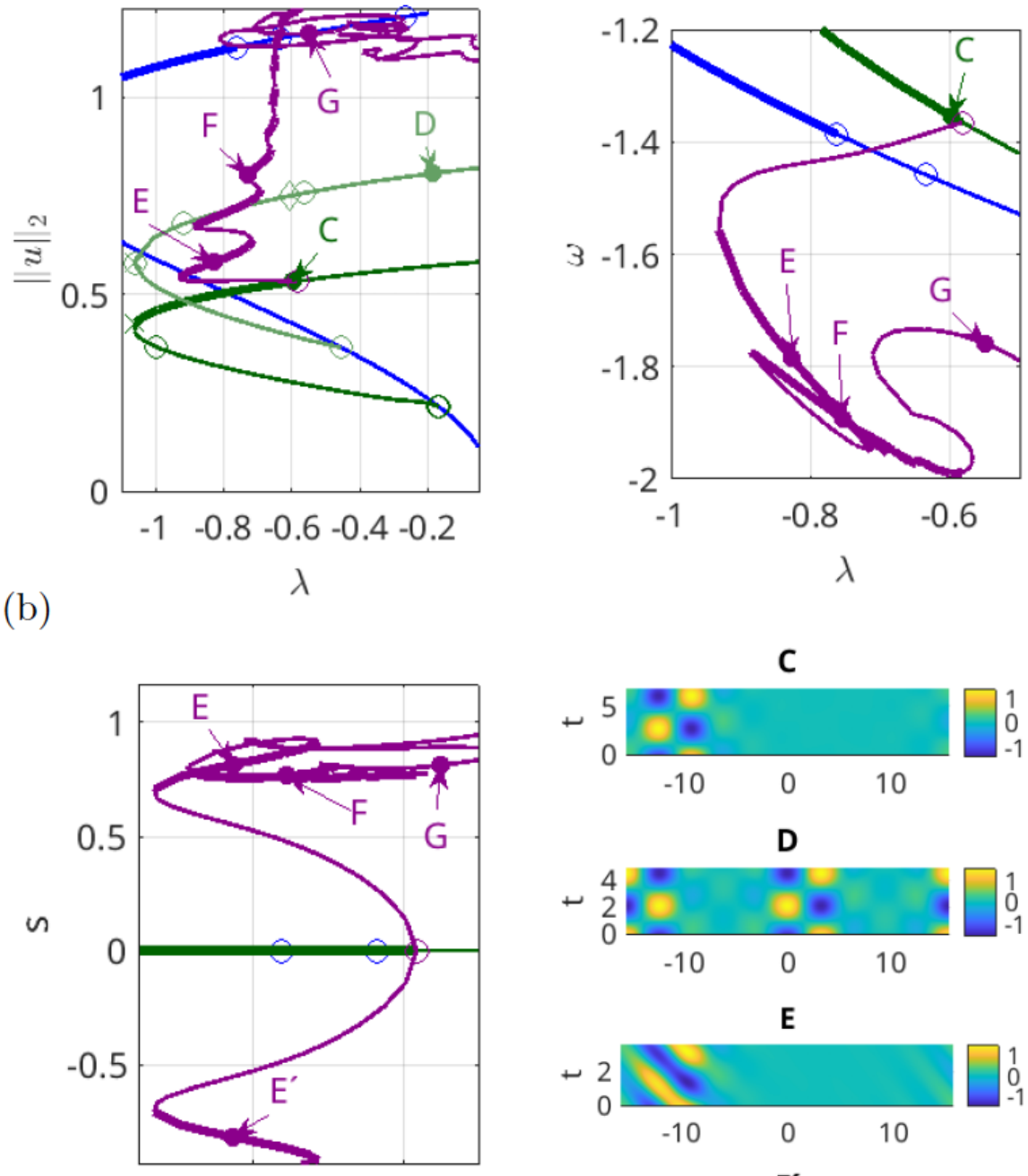

CSHE35: DNS on a larger domain

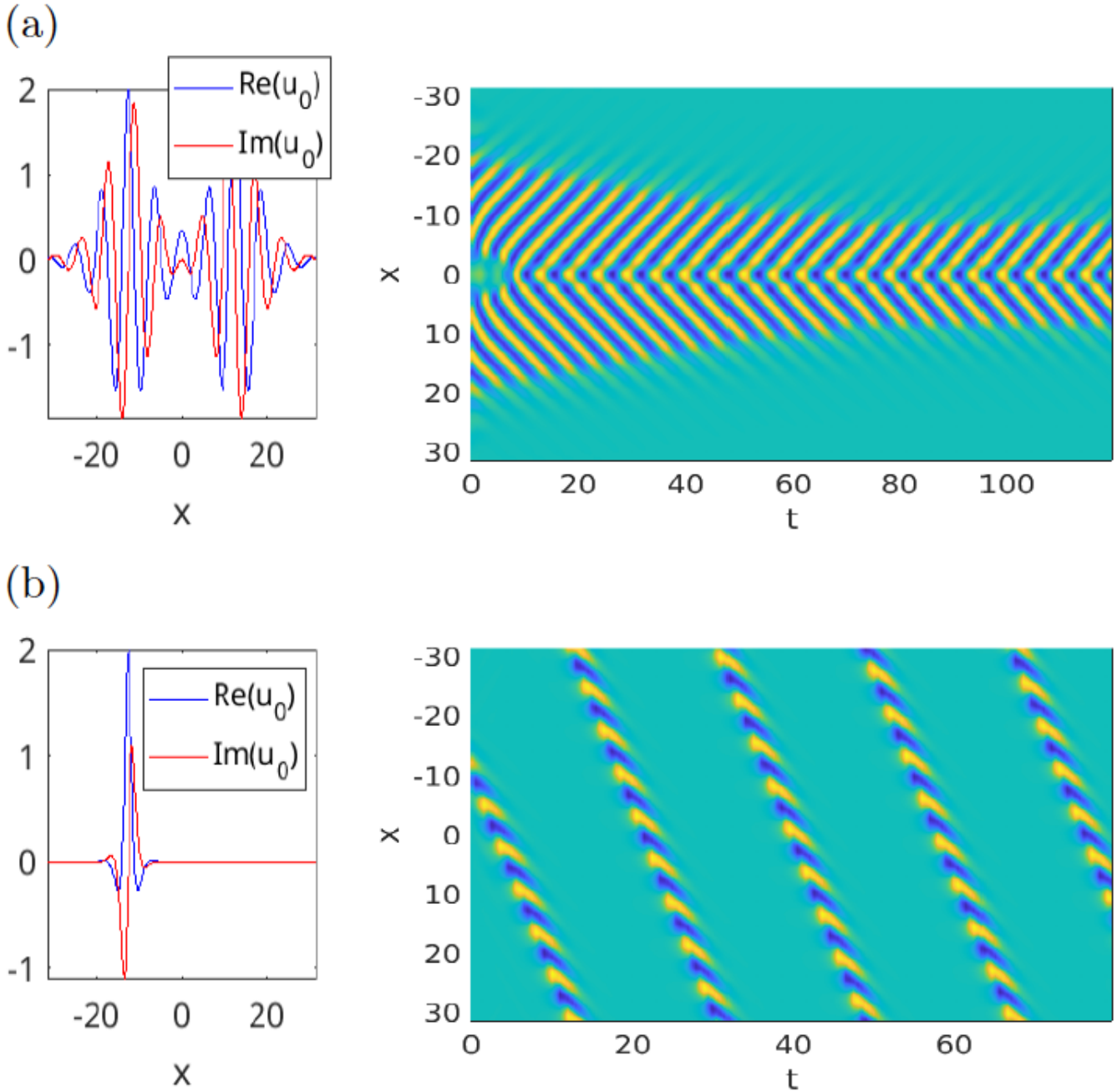

CSHE35 on a disk: RW and SW

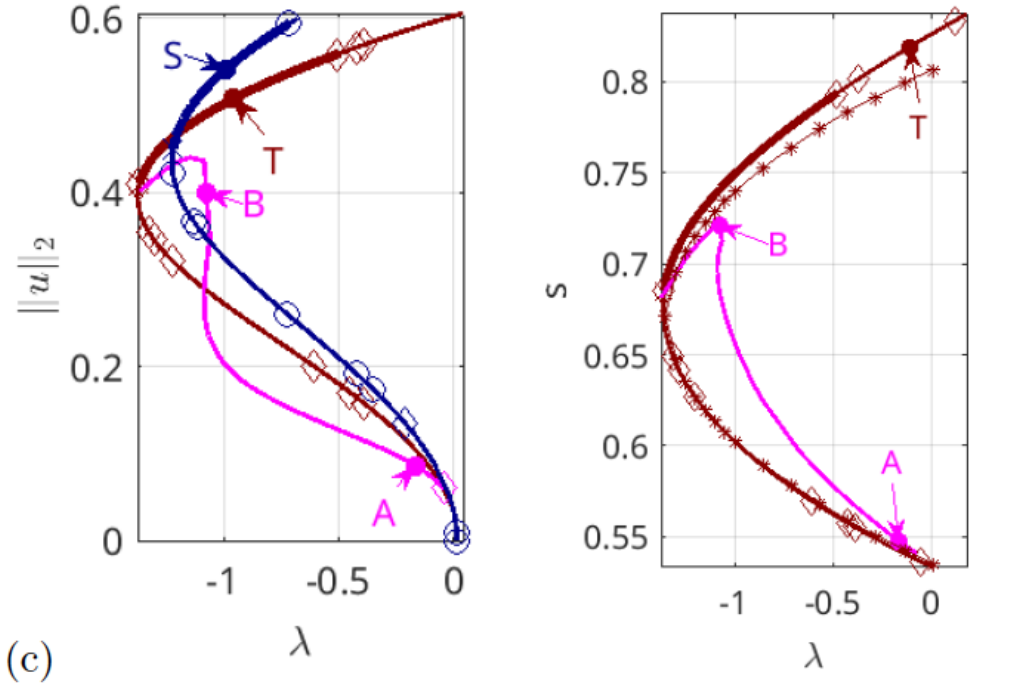

(c)

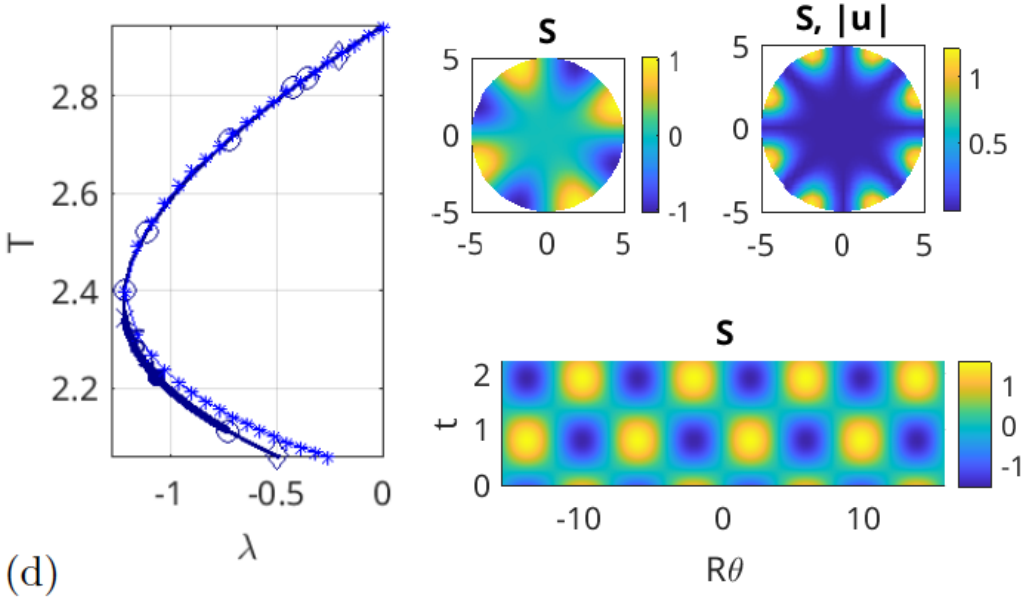

(d)

CSHE35 on a disk: LRW

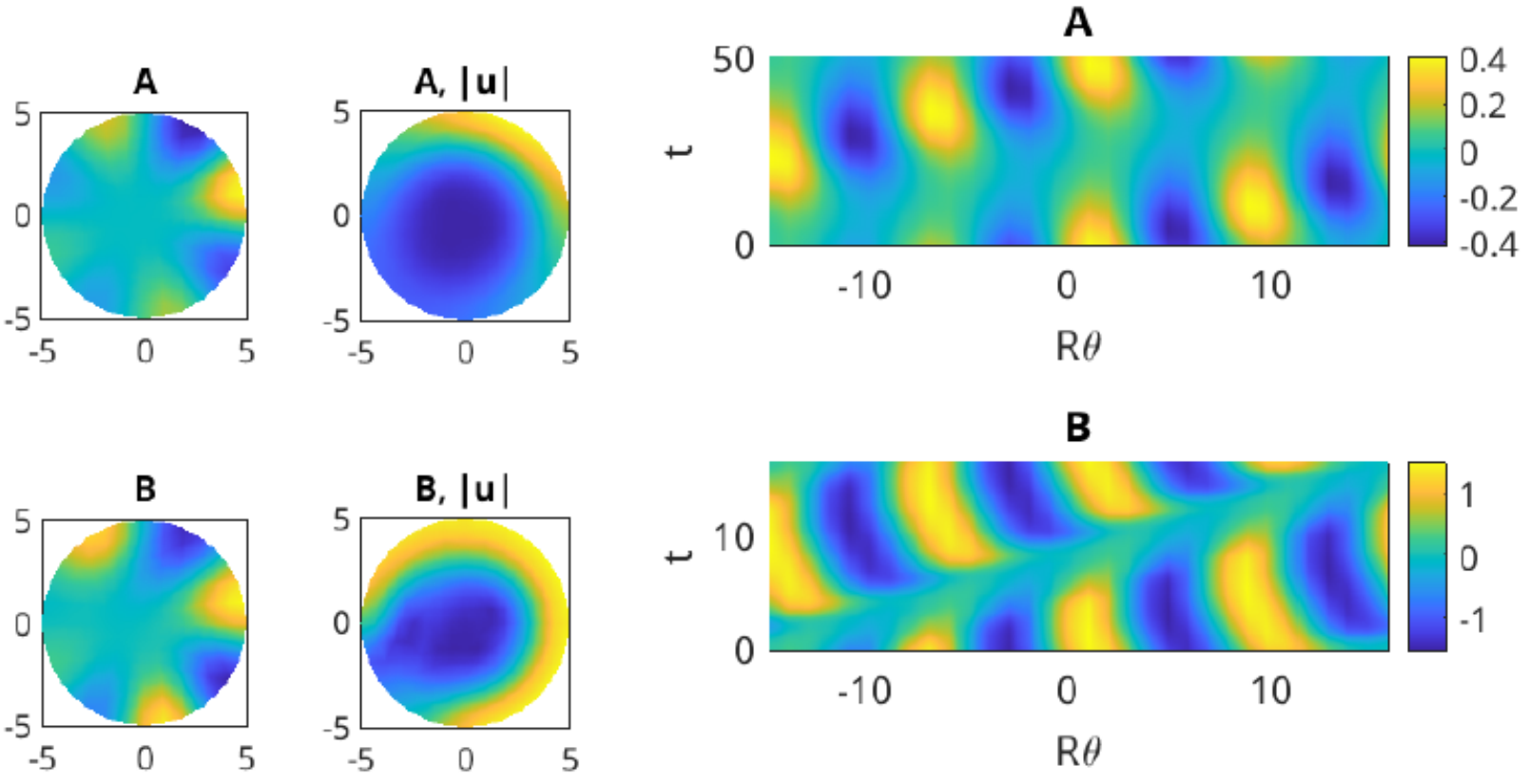

Uecker et al., preprint

CSHE35 on a disk: LSW and rungs

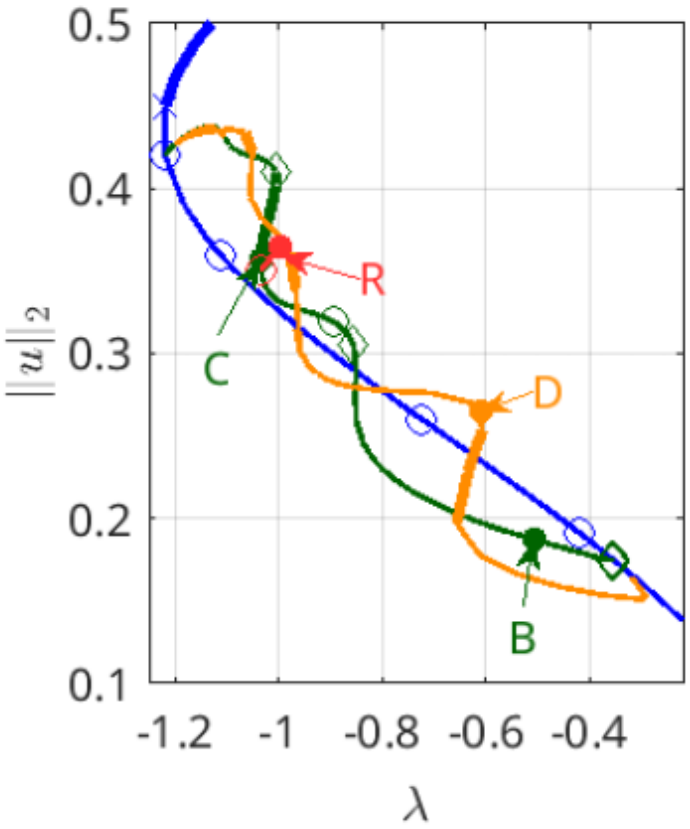

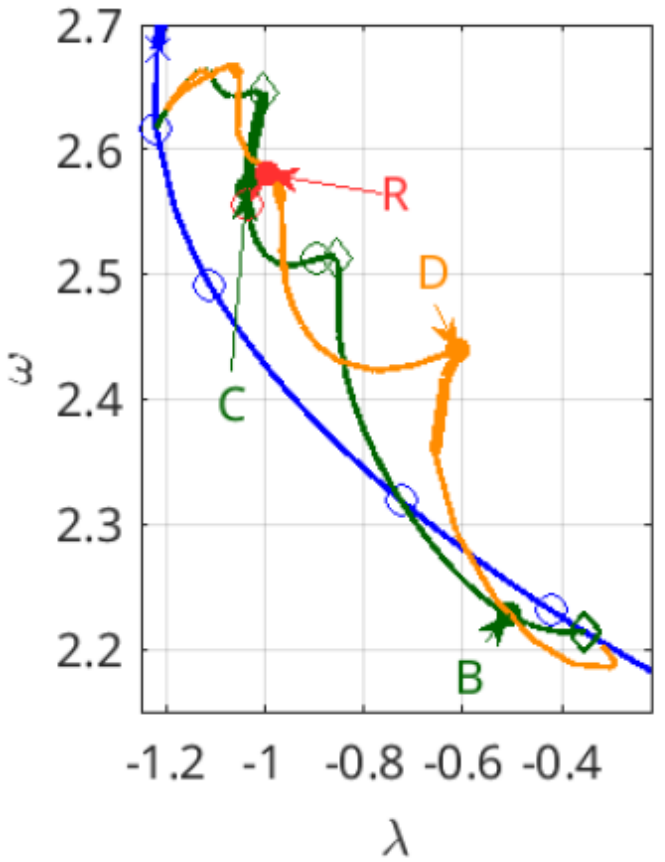

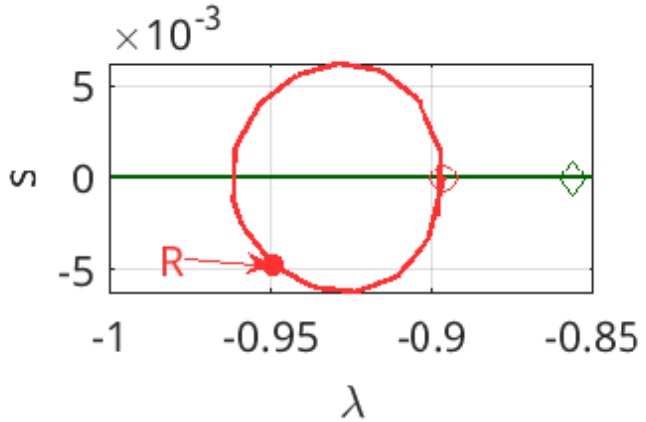

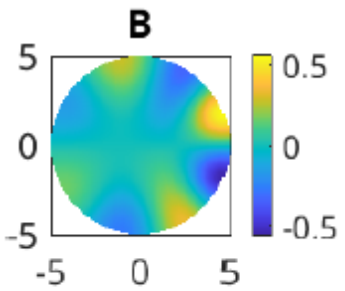

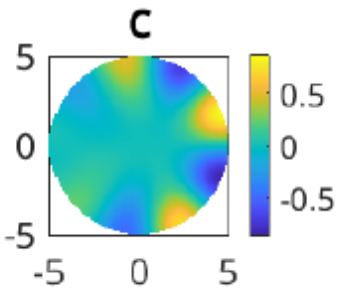

CSHE35 on a disk: wall and bulk states

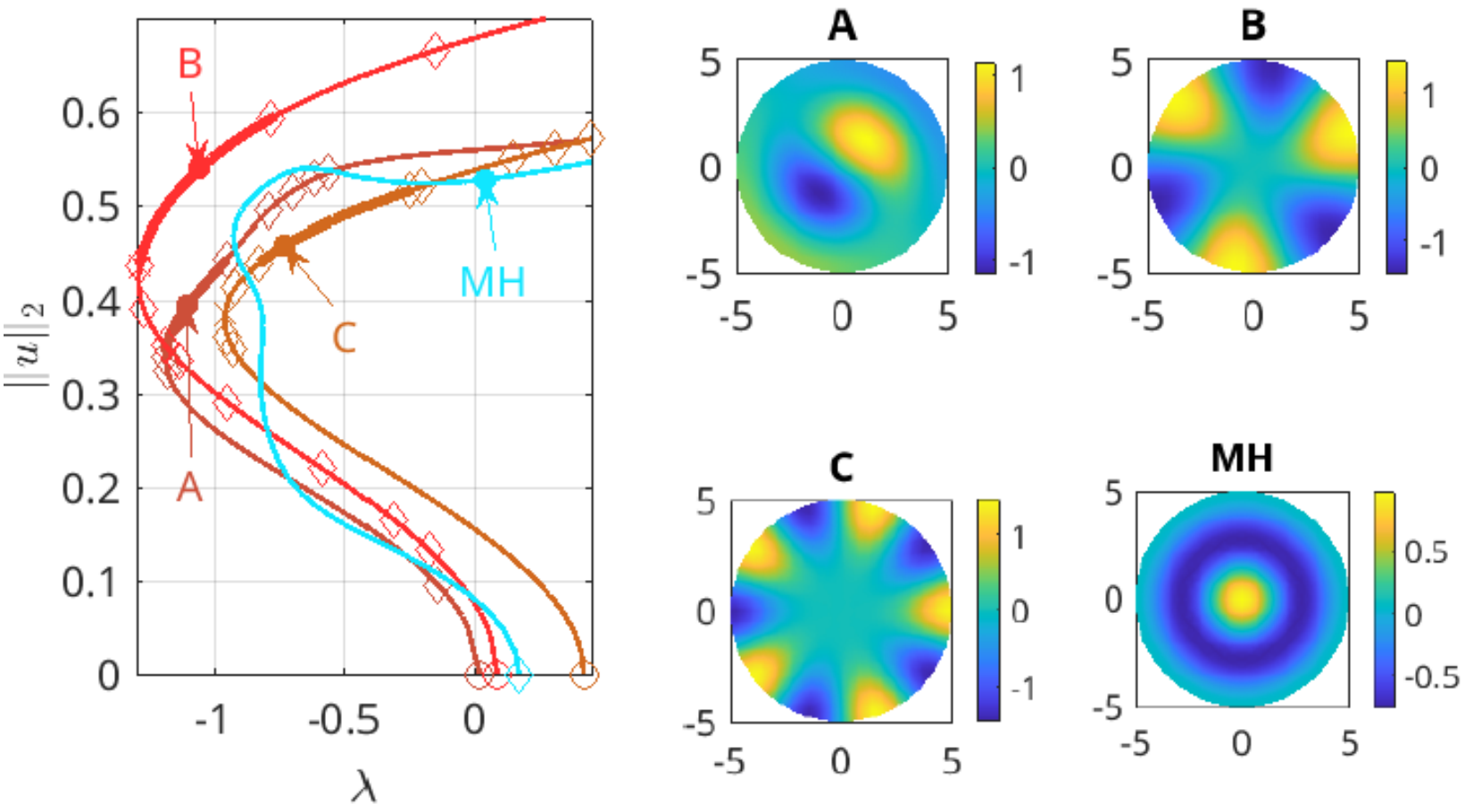

Uecker et al., preprint

CSHE35 on a disk: wall and bulk states

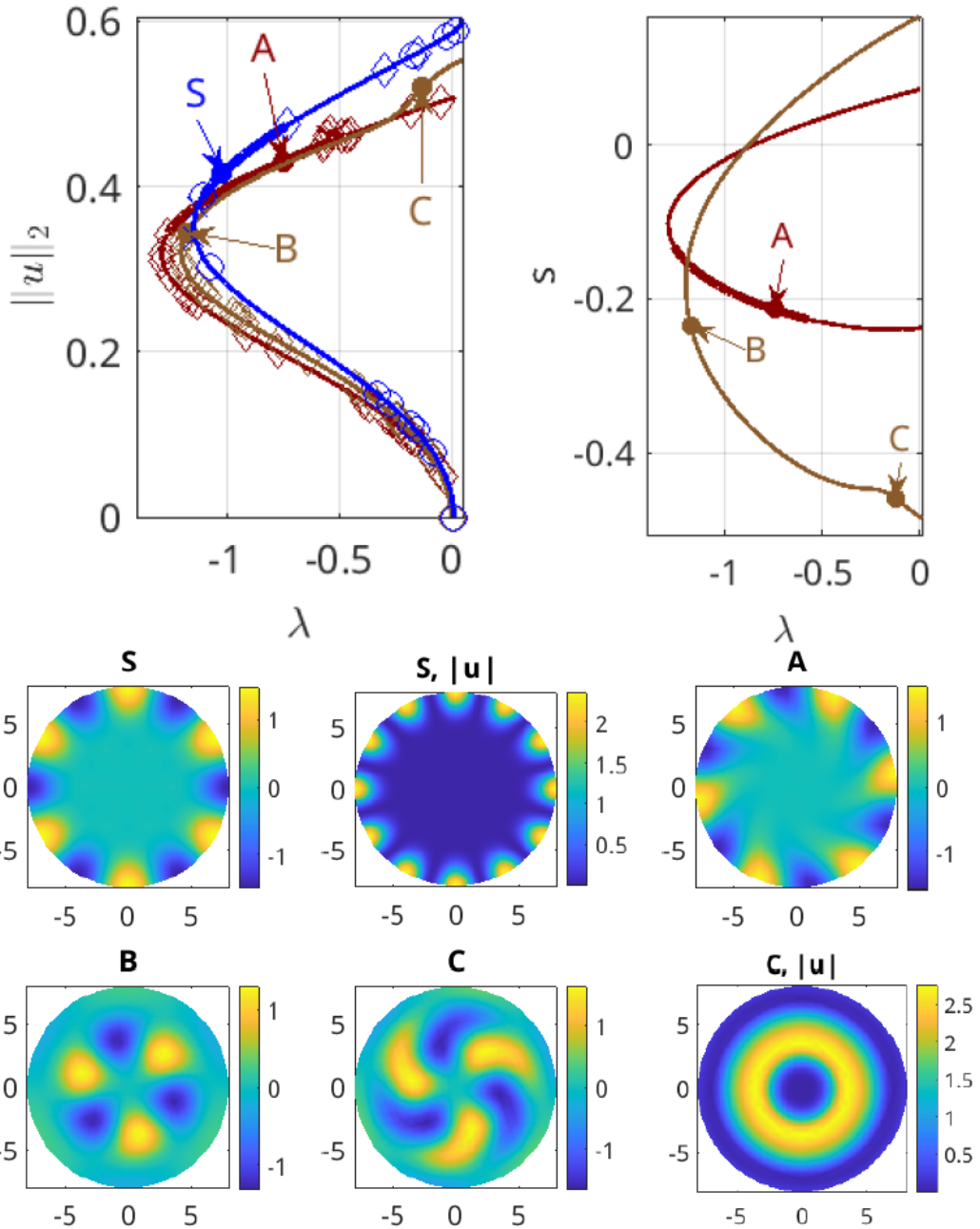

CSHE35 on a disk: wall states

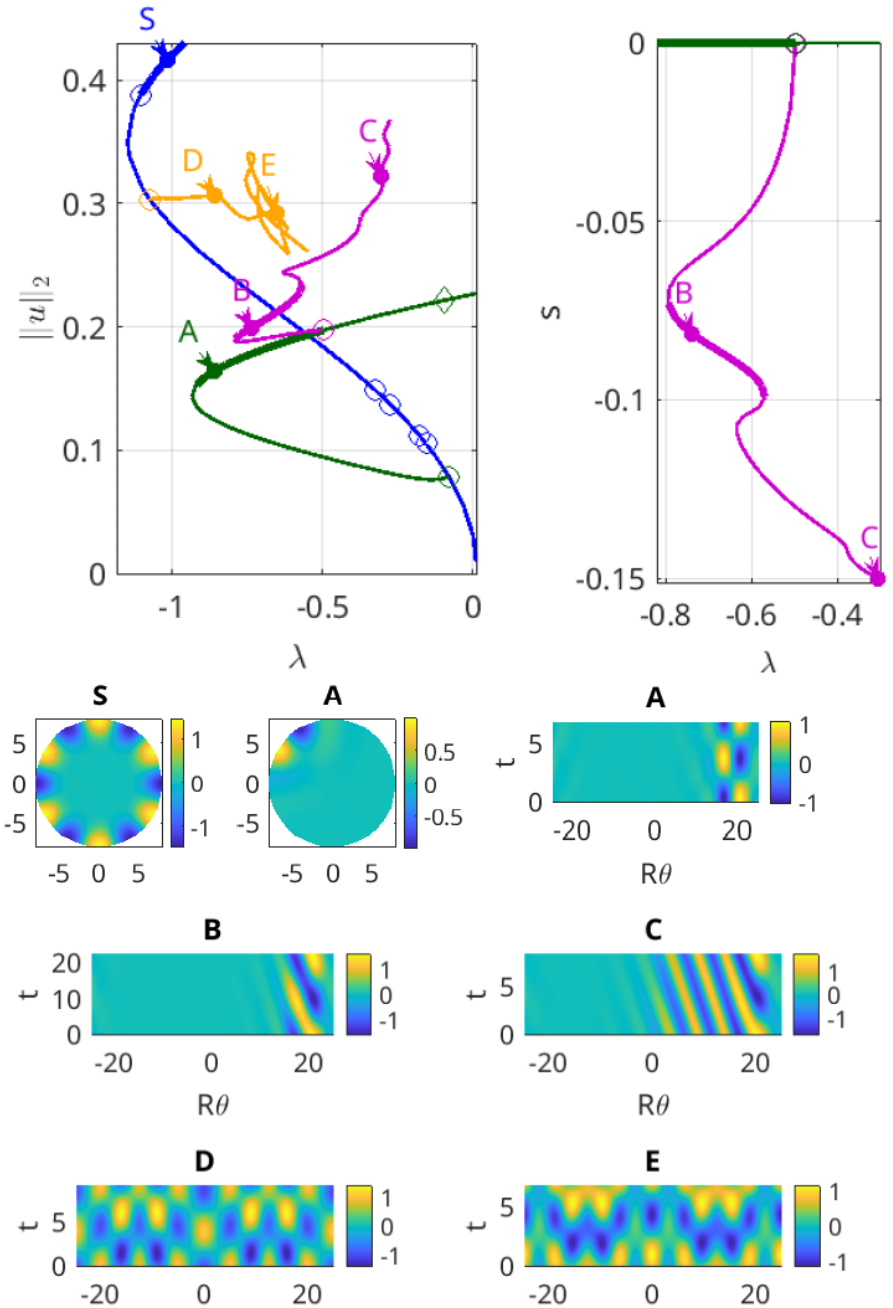

CSHE35 on a disk: DNS

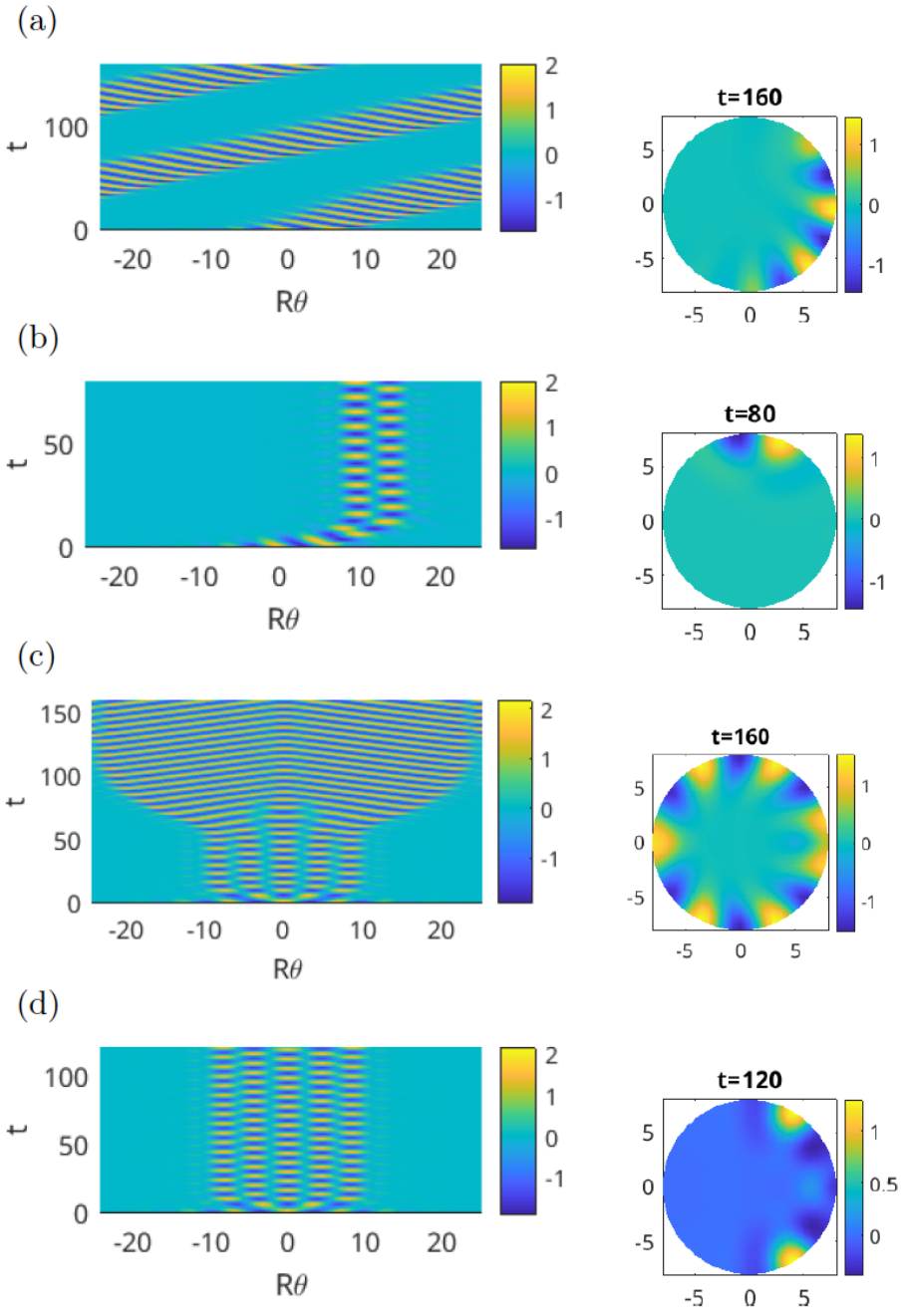

Reaction-diffusion system

Purwins model

$$\begin{aligned} \partial_t u &= k_1 + k_2 u - u^3 - k_3 v - k_4 w + D_u \nabla^2 u, \\ \theta \partial_t v &= u - v + D_v \nabla^2 v, \\ \vartheta \partial_t w &= u - w + D_w \nabla^2 w, \end{aligned}$$

subject to NBCs. We are interested in solutions in the form of jumping oscillons (JOs)

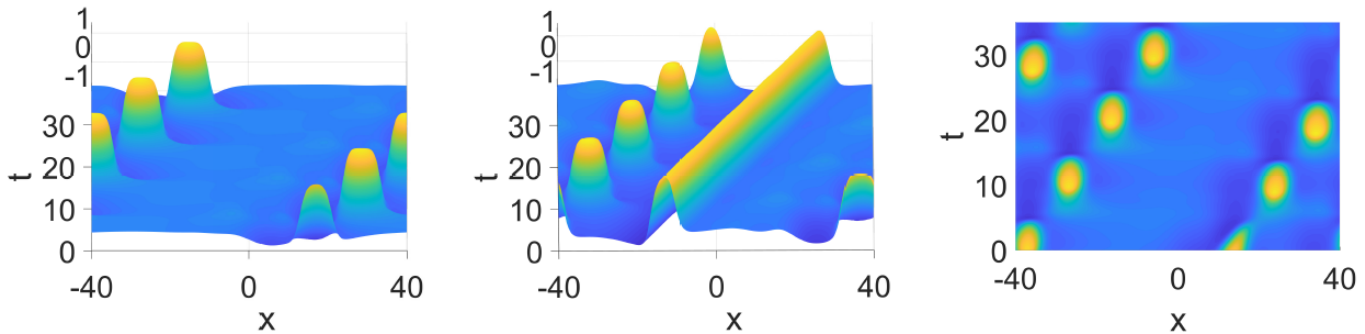

Figure 1. *Space-time profiles of a jumping oscillon (1JO, left panel), a bound pair of a jumping oscillon and a traveling pulse (1JP-1TP, middle panel) and a bound pair of jumping oscillons (2JO, right panel). Reused from [29].*

Wave instability occurs at $k_1 = -7.585$ and creates subcritical TW/SW. Are the JOs related to this instability?

SW and LSW

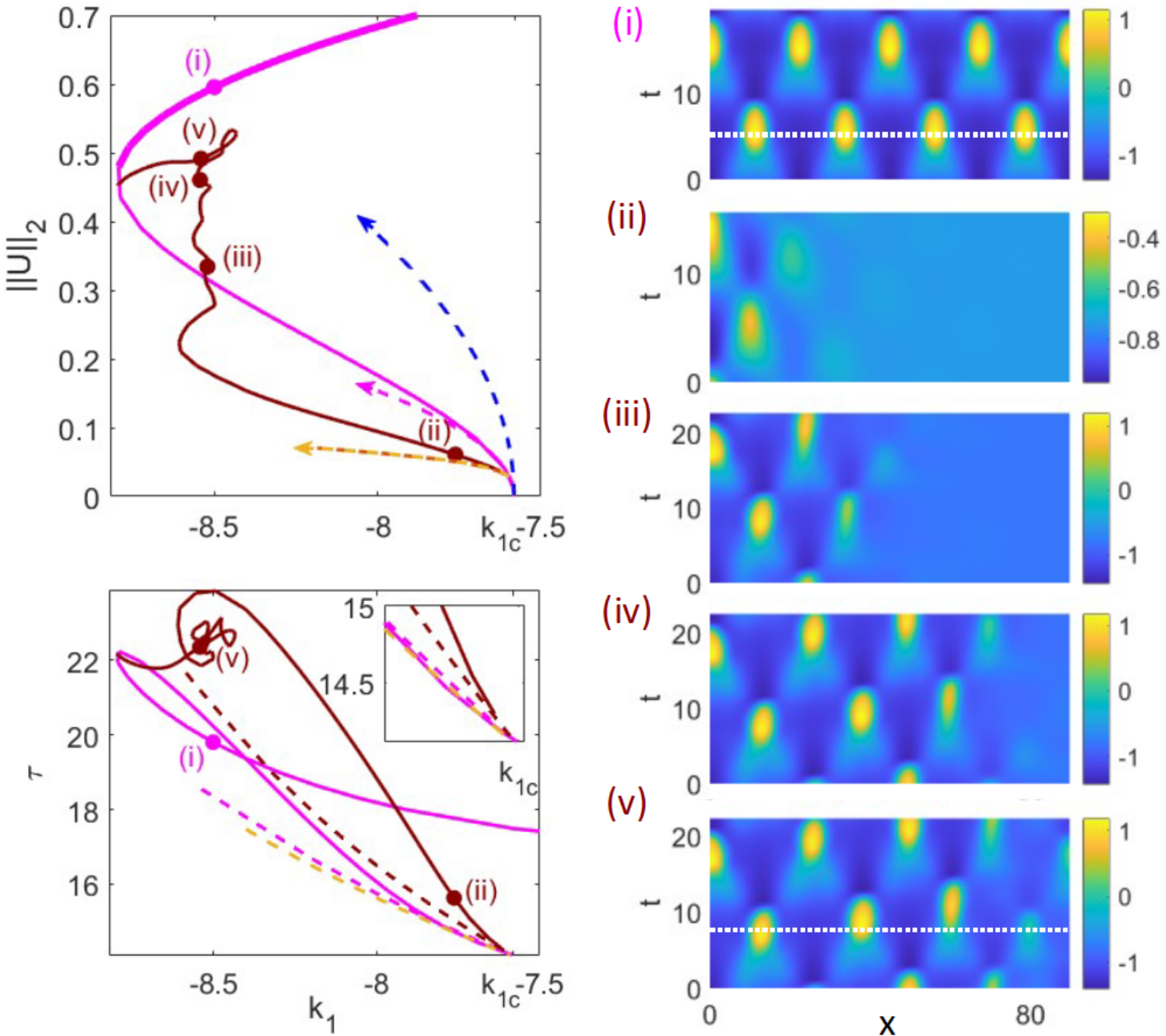
0.7
0.6
0.5
0.4
0.3
0.2
0.1
0
$\|U\|_2$
(i)
(v)
(iv)
(iii)
(ii)
-8.5
-8
k_{1c}-7.5
22
20
18
16
τ
15
14.5
k_{1c}
k_1
(i)
(ii)
(iii)
(iv)
(v)
t
x
0
10
20
80
1
0
-1
-0.4
-0.6
-0.8

Weakly nonlinear theory: CCGLE with $S_g \neq 0$

We use an exact solution of the CCGLE for $S_g = 0$, $A_{\mathrm{LSW}} = \Lambda e^{i\Omega_{\mathrm{LSW}} t} \mathrm{sech}^{1+i\Theta} Kx$, to initialize continuation in the group velocity S_g:

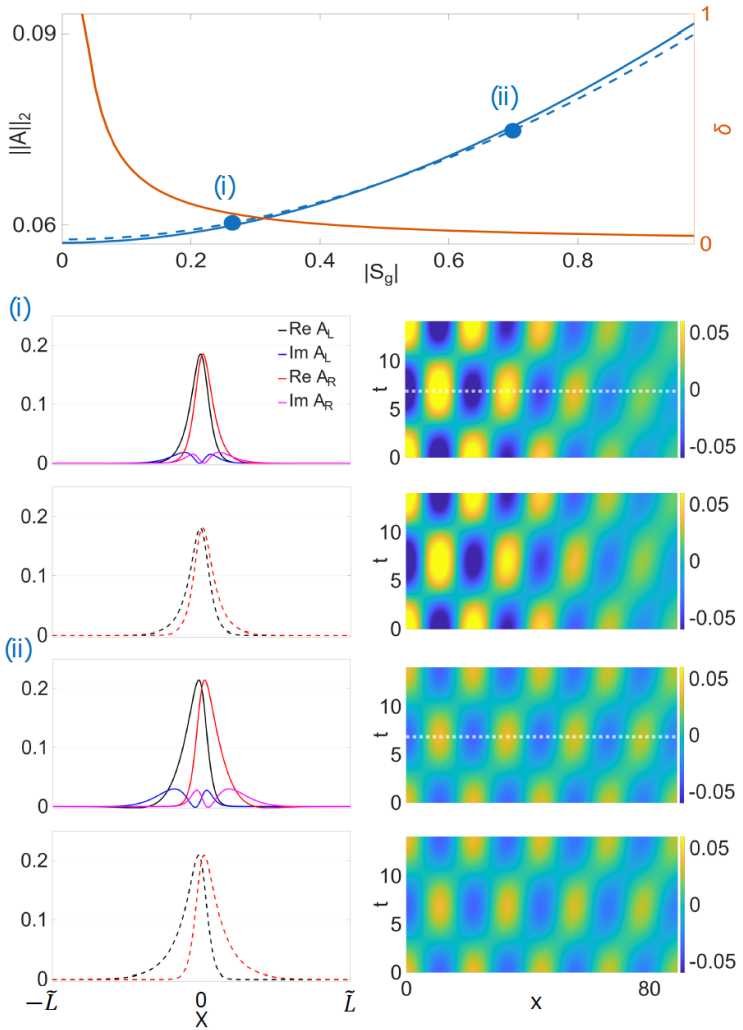

Traveling pulses and JOs

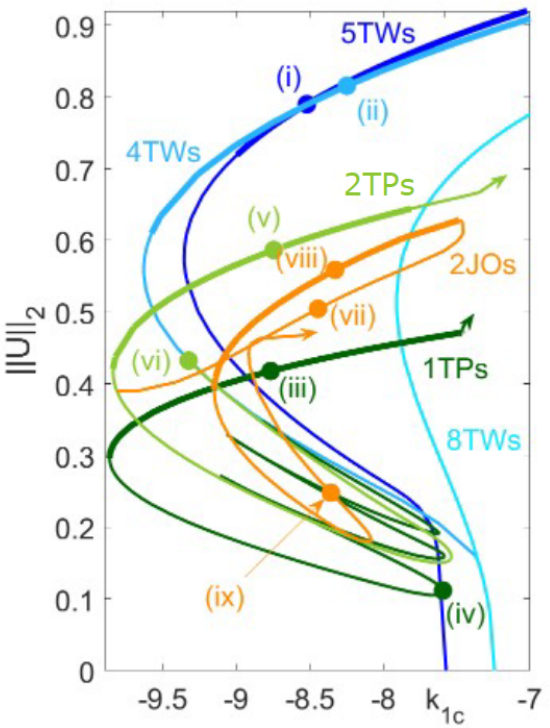

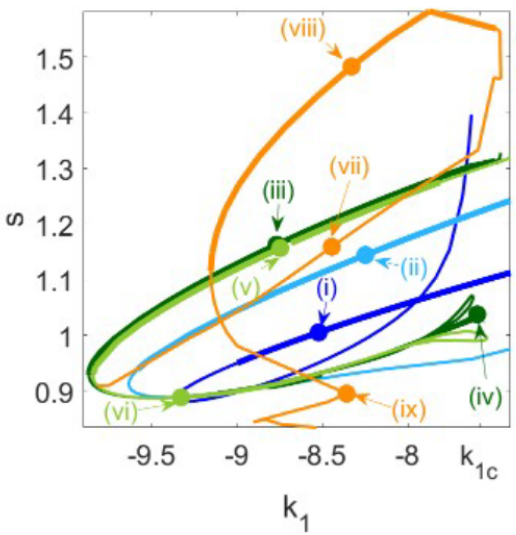

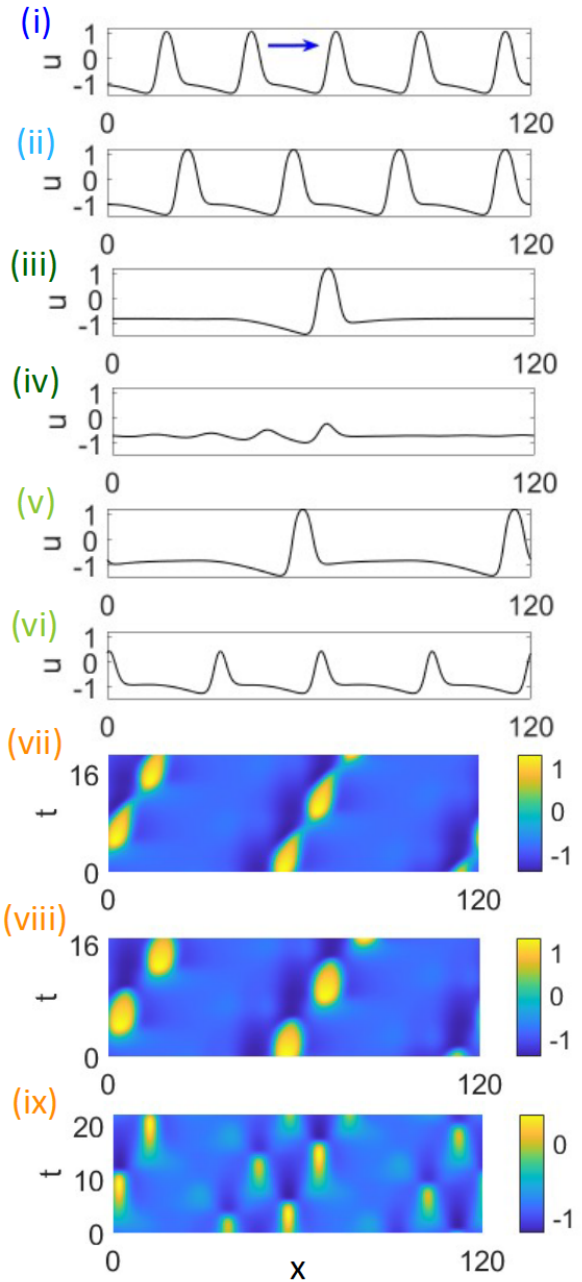

Snaking of traveling pulses and DNS

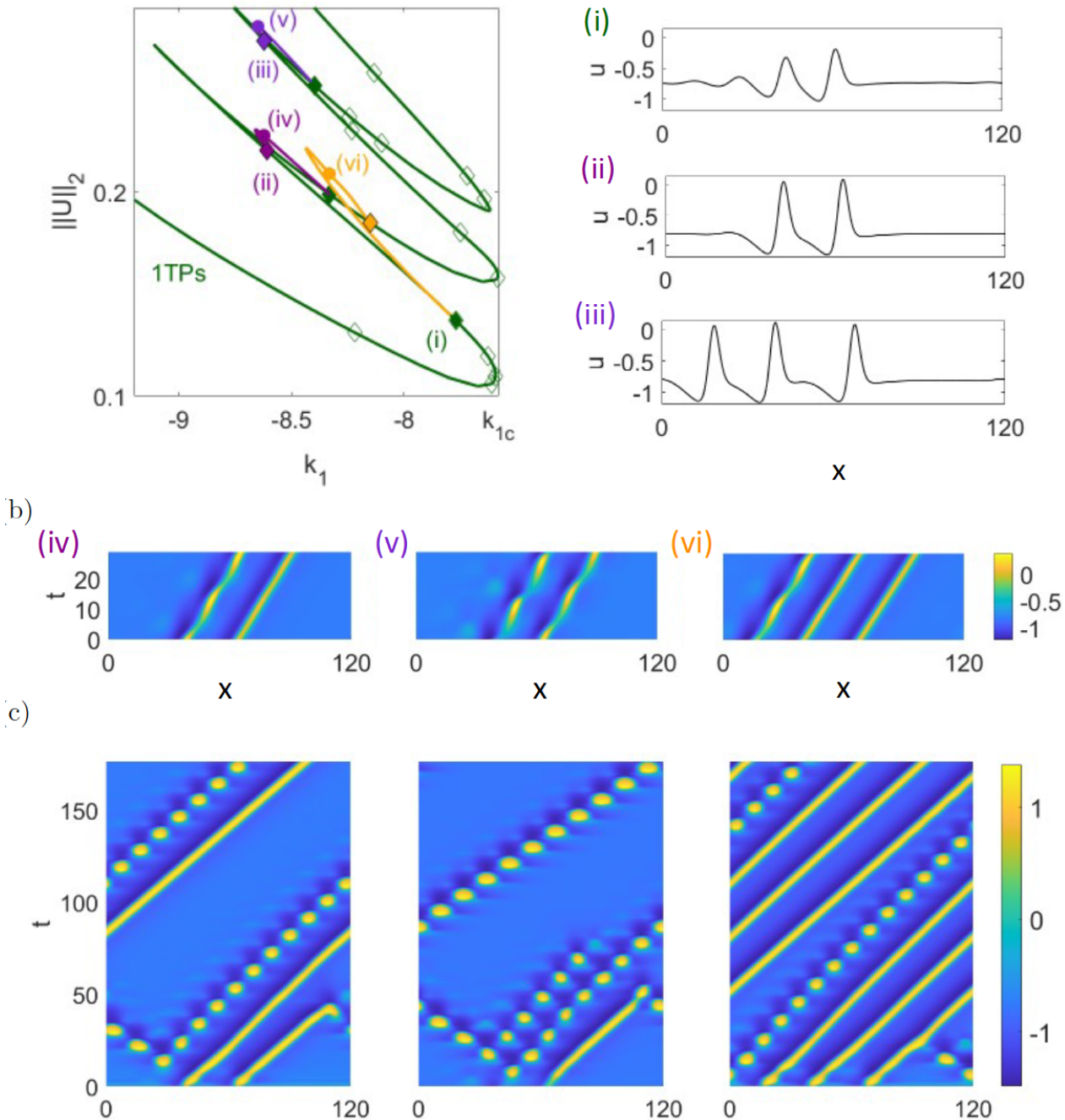

Snaking of traveling pulses

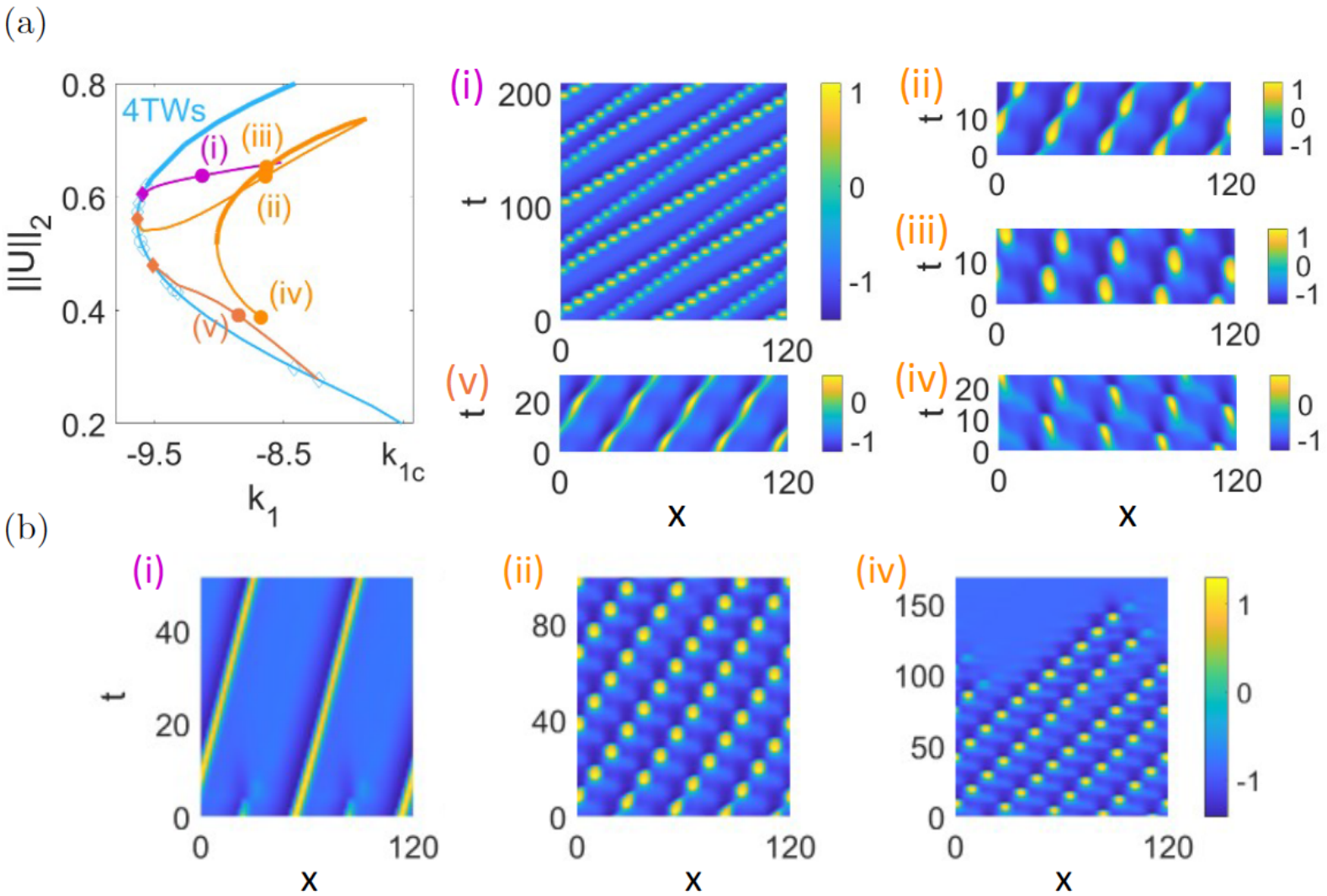

Knobloch et al., preprint

Snaking of traveling pulses: large domain

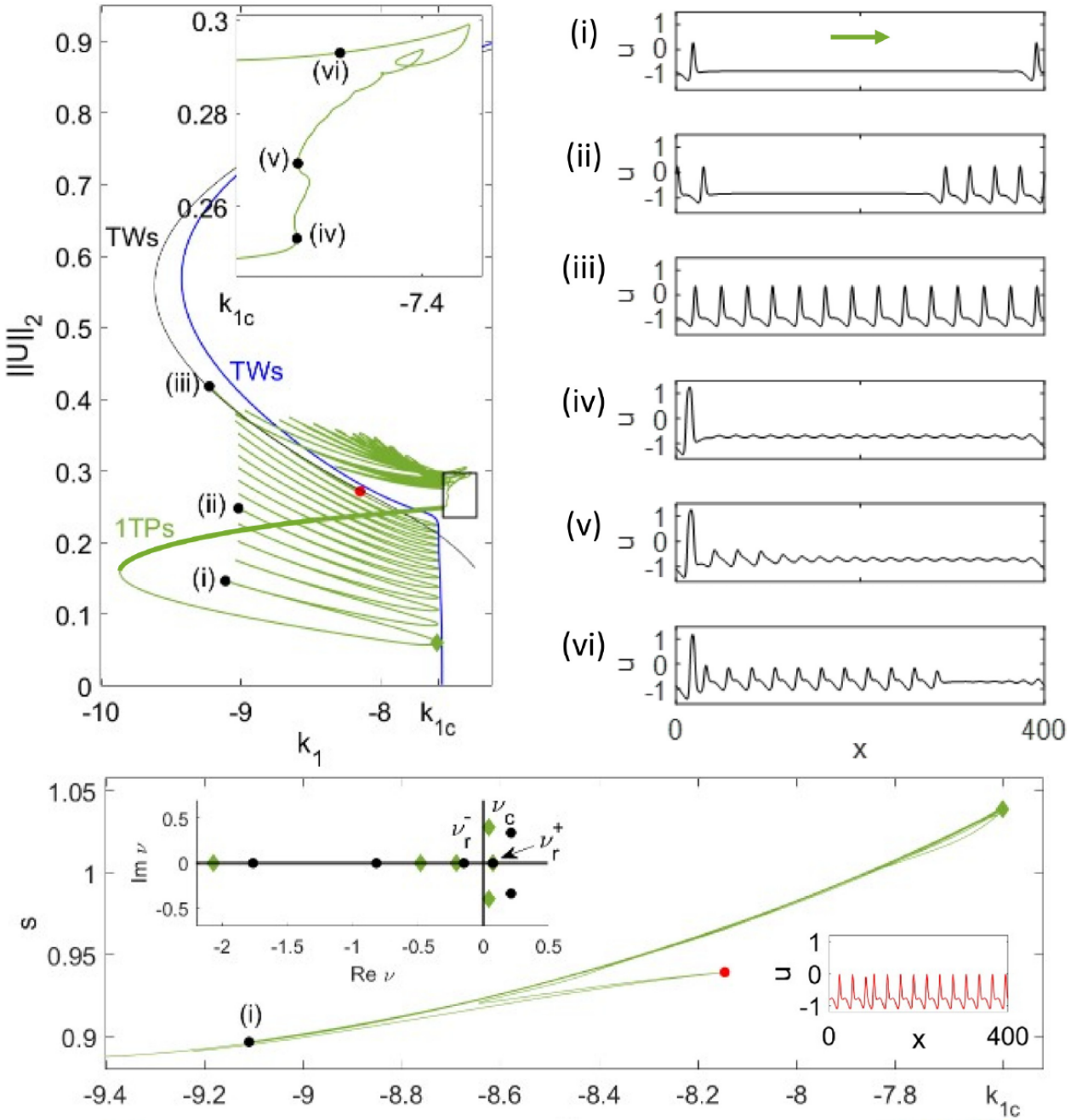

Purwins model on a disk: $R = 20$

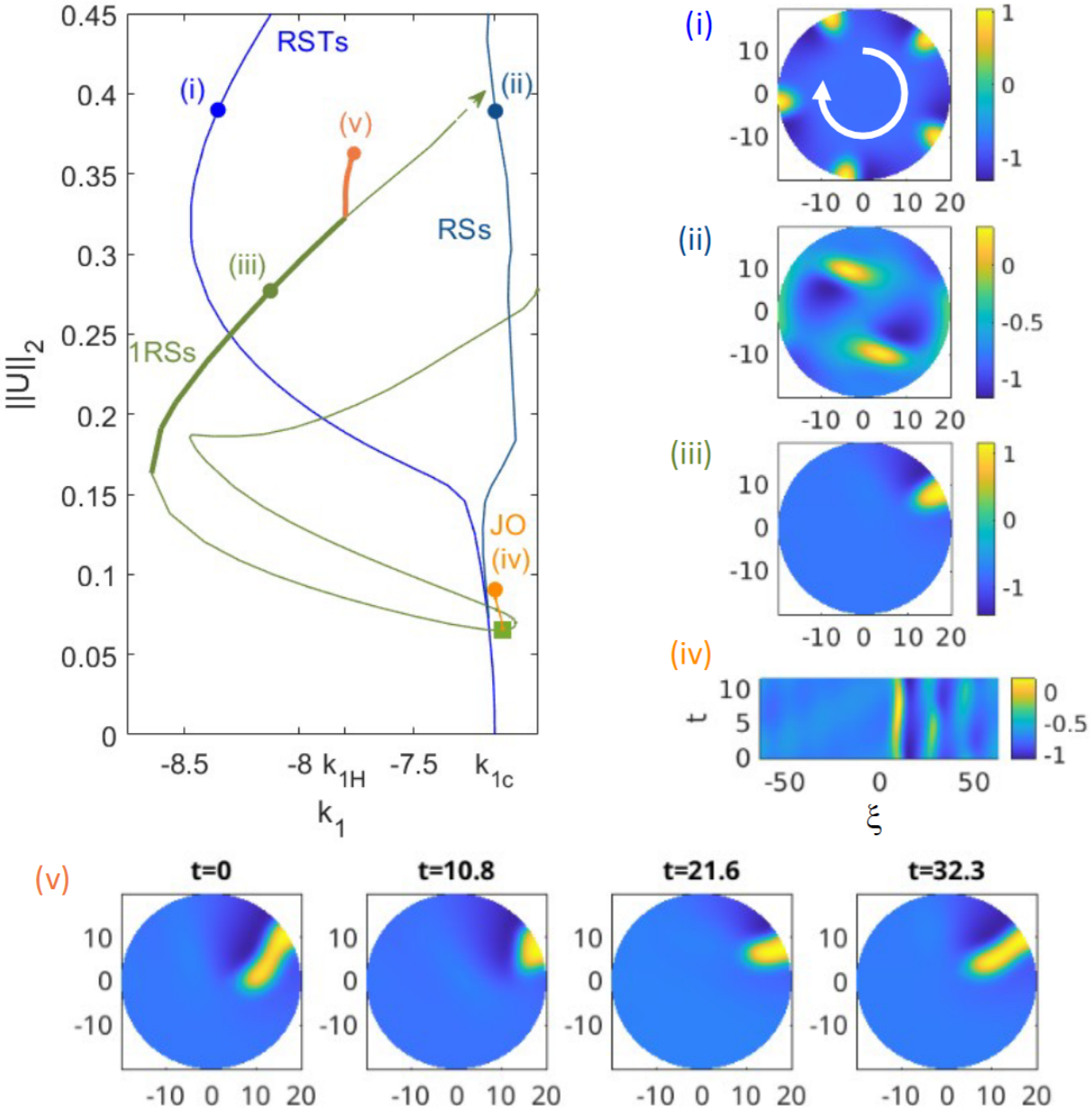

DNS on a disk: $R = 20$

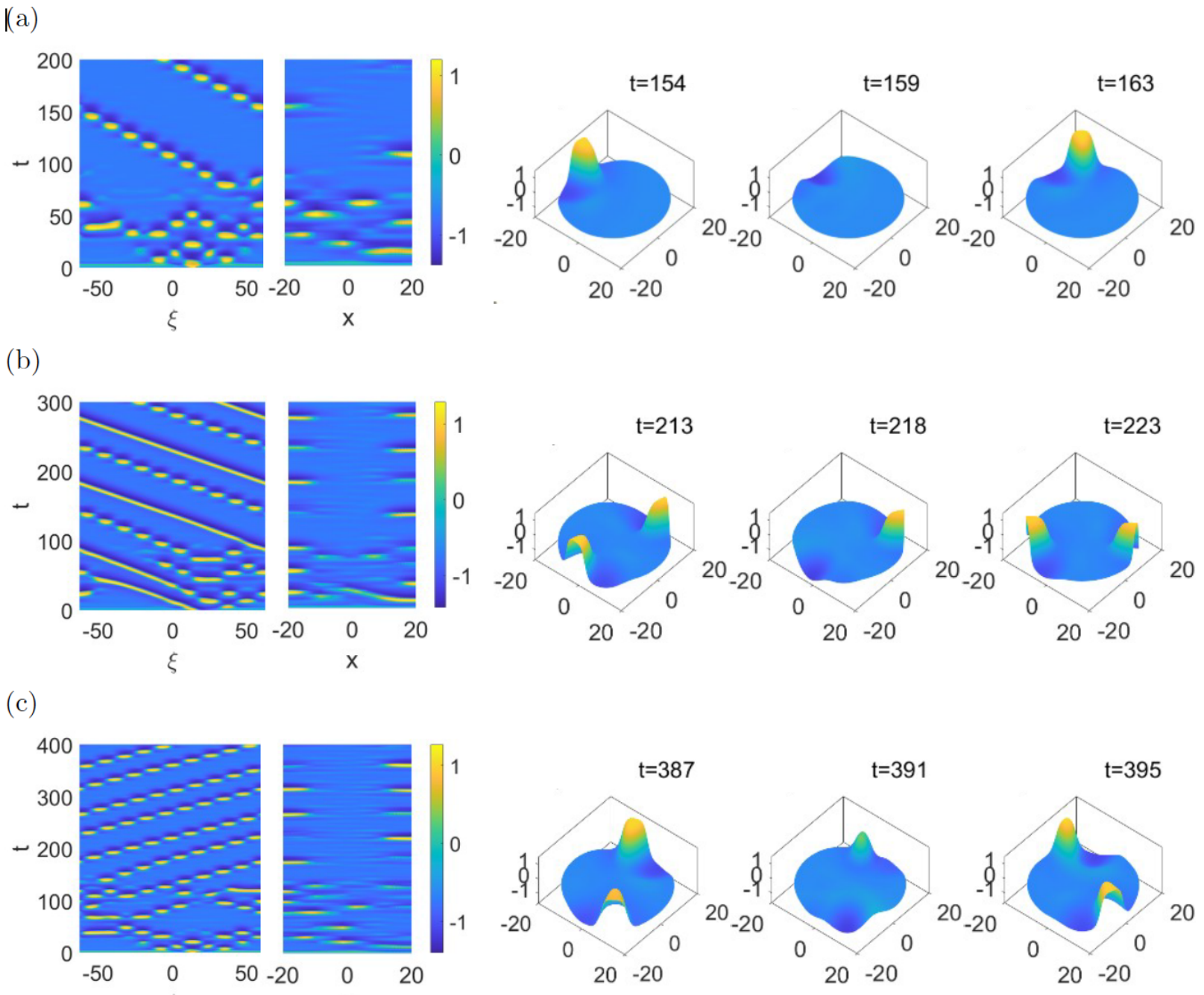

Oscillating wall spot: $R = 20$

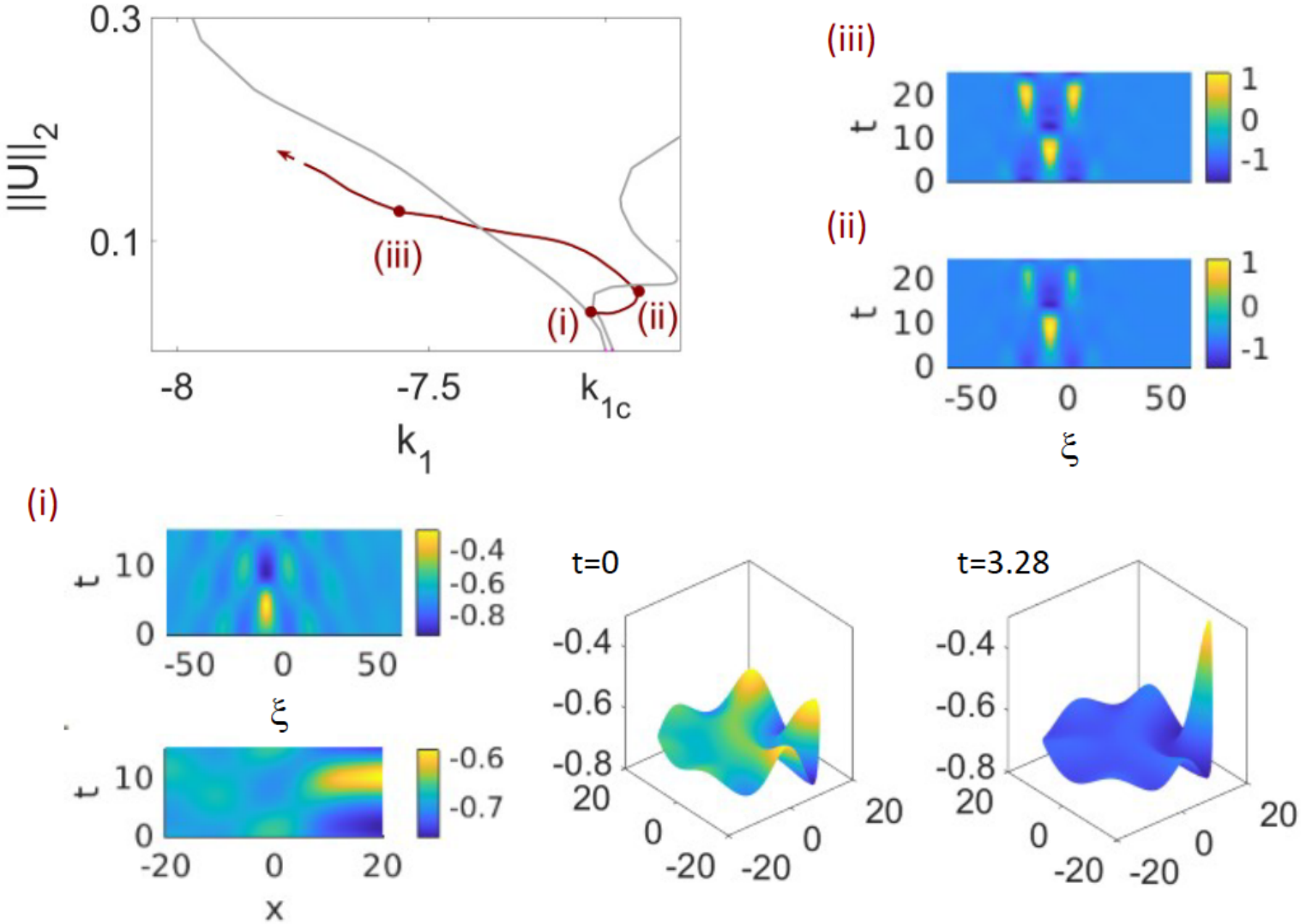

Knobloch et al., preprint

Bifurcation diagram on a disk: $R = 30$

Rotating (blue) ans standing (pink) spot arrays:

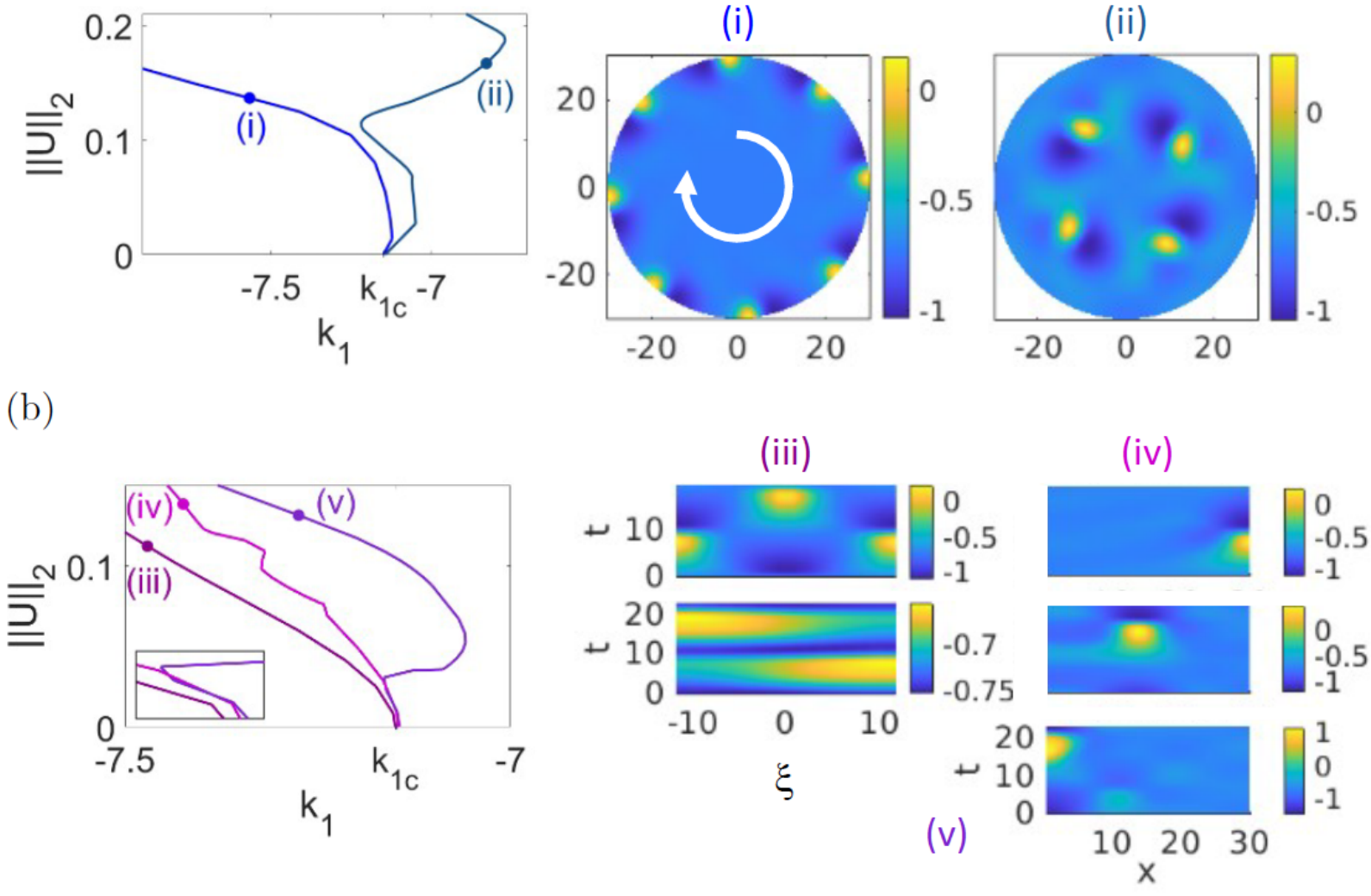

DNS on a disk: $R = 30$

Wall-bulk rotating and oscillating states:

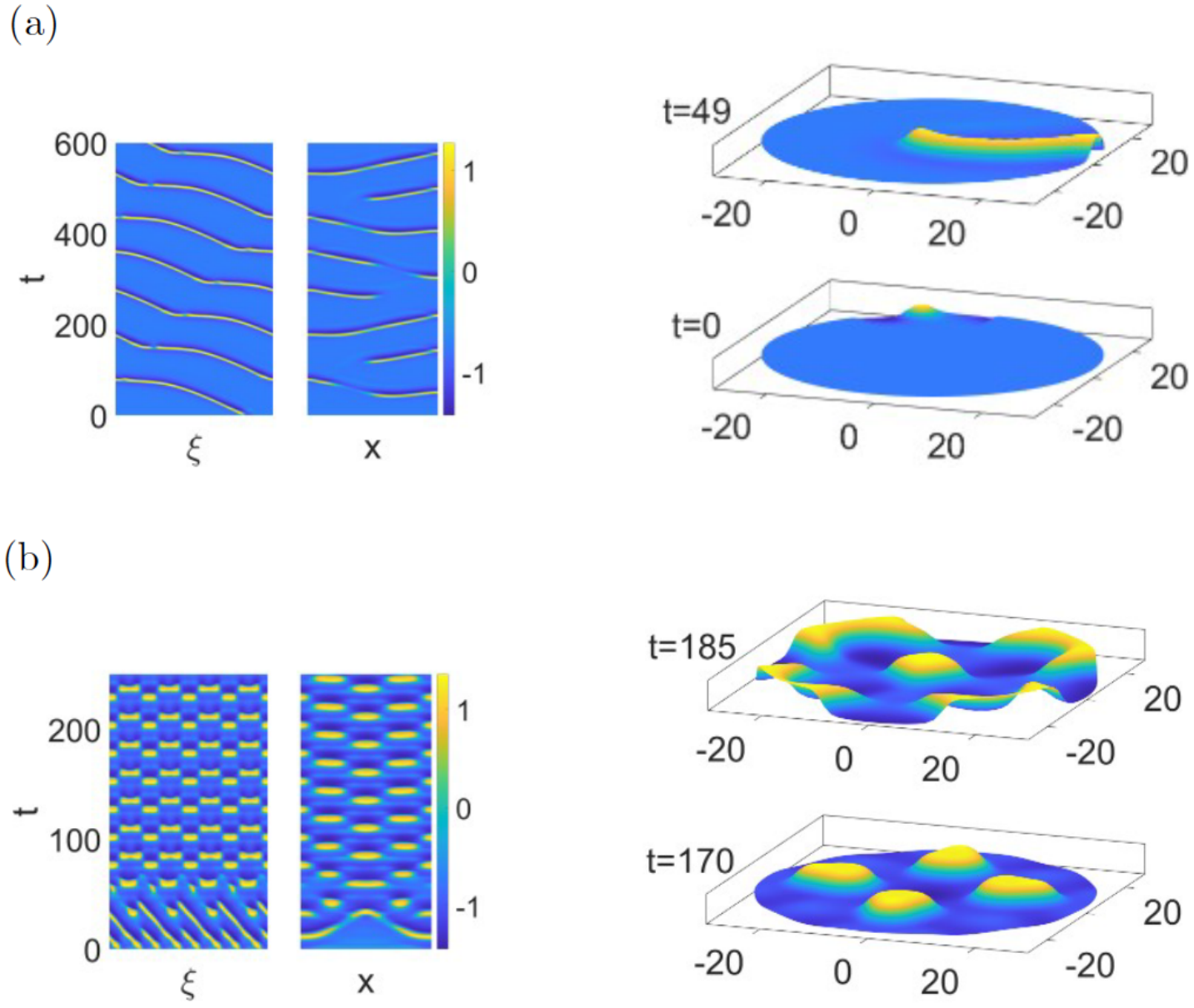

DNS on a disk: $R = 30$

Oscillations with (a) stable, (b) unstable bulk:

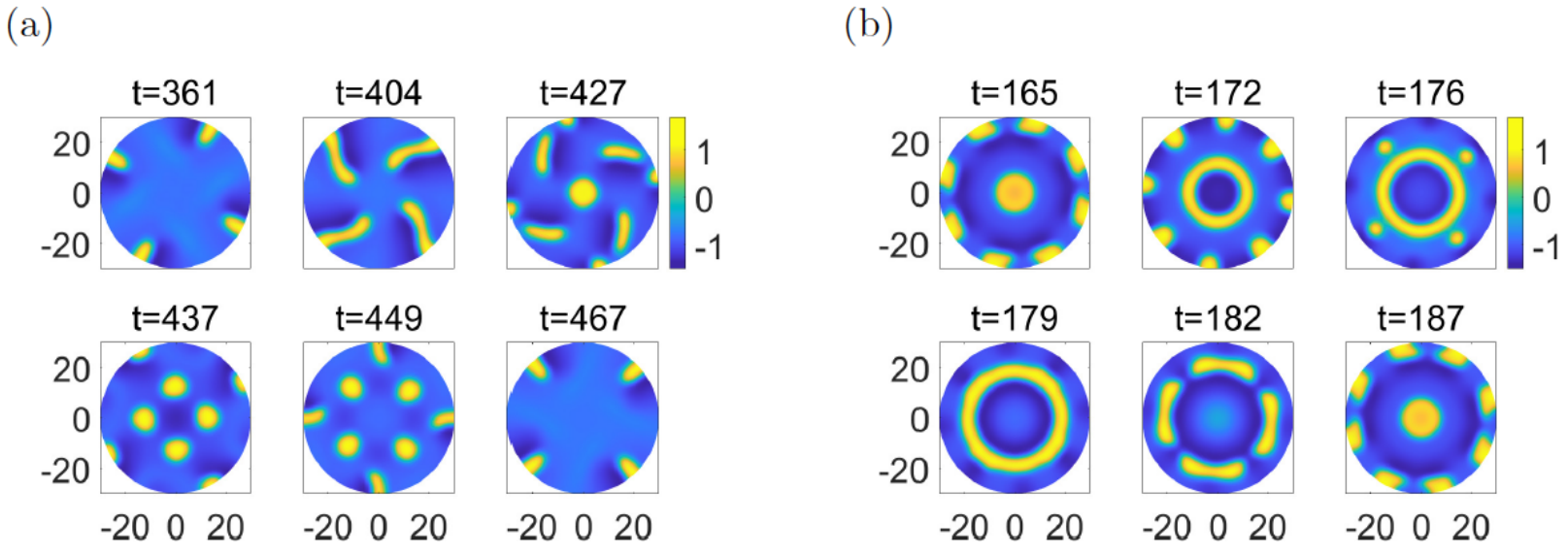

Knobloch et al., preprint

DNS on a disk: $R = 30$

Oscillations with unstable bulk ($k_1 = -7.0 > k_{1c}$):

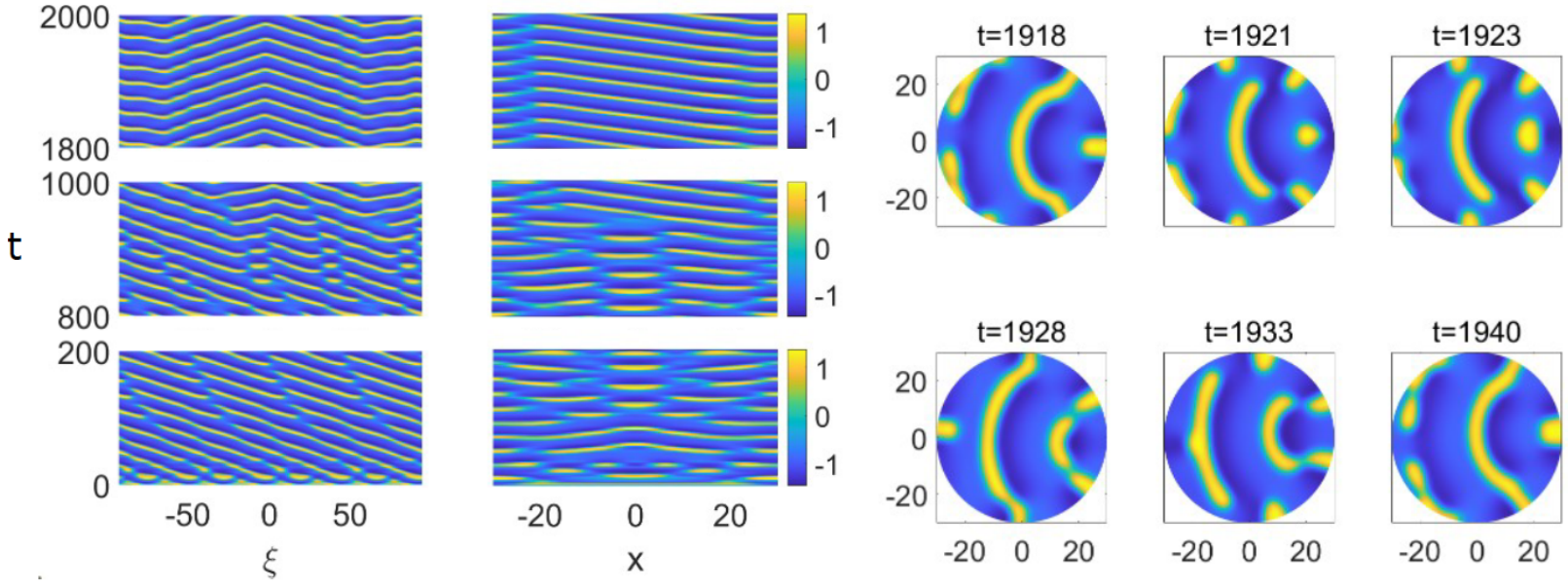

Knobloch et al., preprint

Convection is a spinning cylinder: wall modes precess

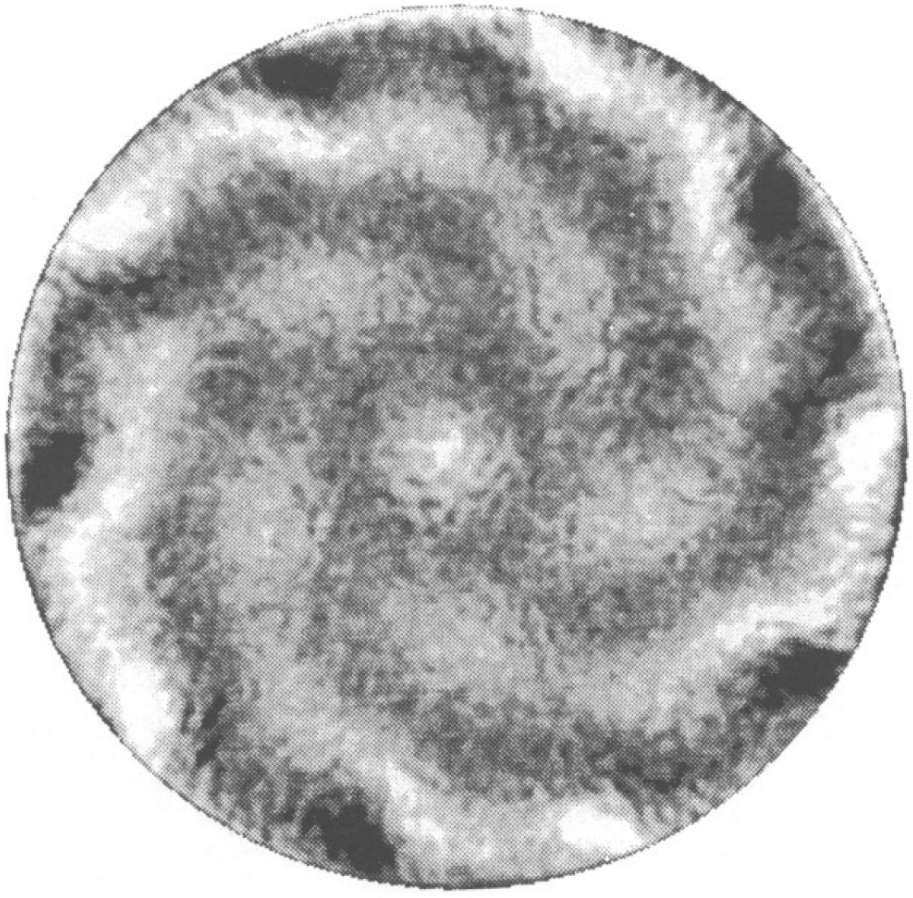

Fig. 4. – Shadowgraph image of the $m = 5$ state for $\Omega = 2145$ and $\varepsilon = 2.6$. The entire pattern precesses in the rotating frame at constant velocity.

Zhong et al., PRL**67** 2473 (1991); Ecke et al., EPL **19**, 177 (1992).

Linear theory: wall modes precess

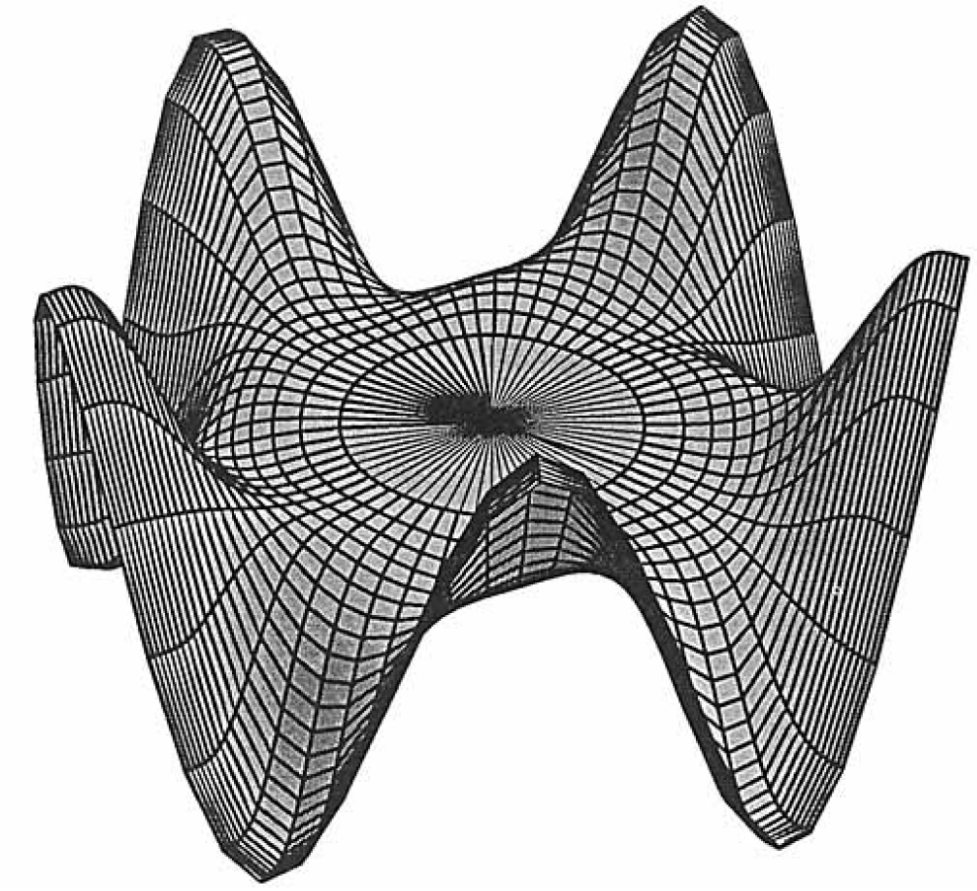

FIGURE 2. A plot of Θ ($z = \frac{1}{2}$) for an $m = 5$ fast mode at $\Omega = 500$, $\sigma = 7.0$ in a $\Gamma = 1$ cylinder, for boundary conditions A. For this mode $R_c^{(5)} = 35989.6$, $\omega_c^{(5)} = 26.884$.

Goldstein et al., JFM **248**, 583 (1993)

Linear theory: wall modes precess

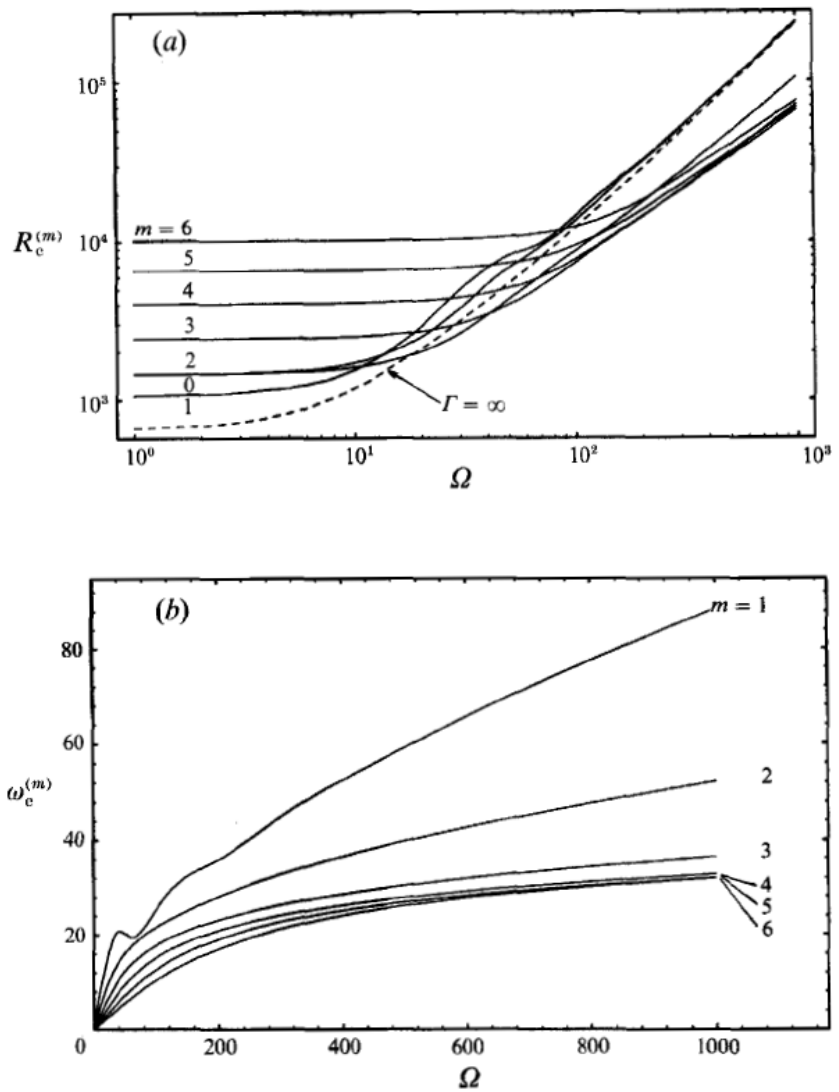

FIGURE 1. The linear stability results for the fast modes in a $\Gamma = 1$ cylinder with boundary conditions A and $\sigma = 7.0$. (*a*) The critical Rayleigh number $R_c^{(m)}$ and (*b*) the onset precession frequency $\omega_c^{(m)}$ as functions of the rotation rate Ω for several different values of the azimuthal wavenumber m. The dashed line in (*a*) indicates the corresponding result for an unbounded plane layer (Chandrasekhar 1961).

Linear theory: bulk modes also precess

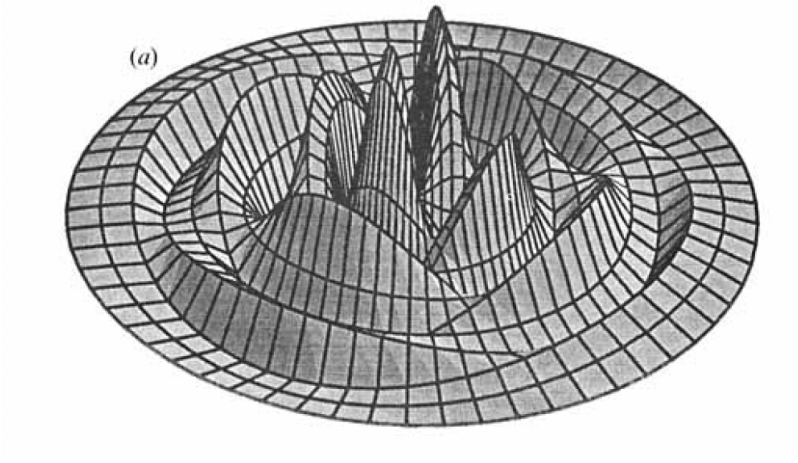

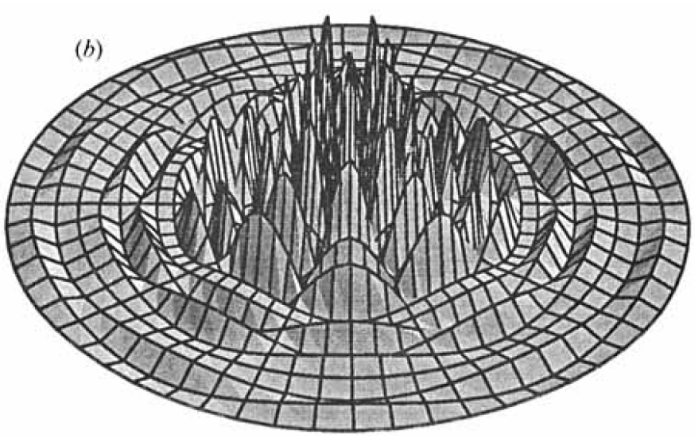

$m = 2$, $\Gamma = 1.84$ $m = 5$, $\Gamma = 4.39$

The wall and bulk modes display very different behavior with respect to the domain aspect ratio Γ:

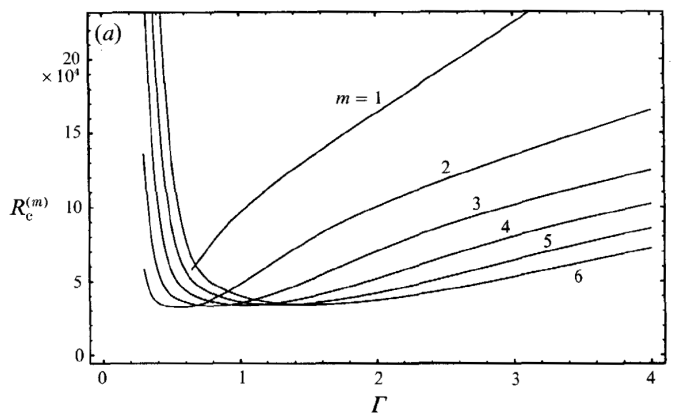

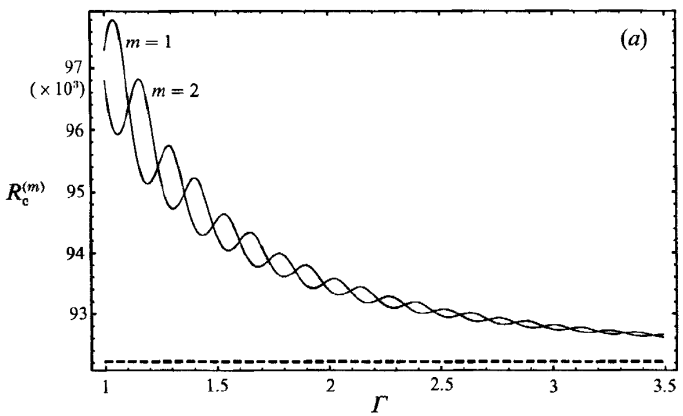

Goldstein et al., JFM **248**, 583 (1993)

Convection in a spinning cylinder: robust boundary flow

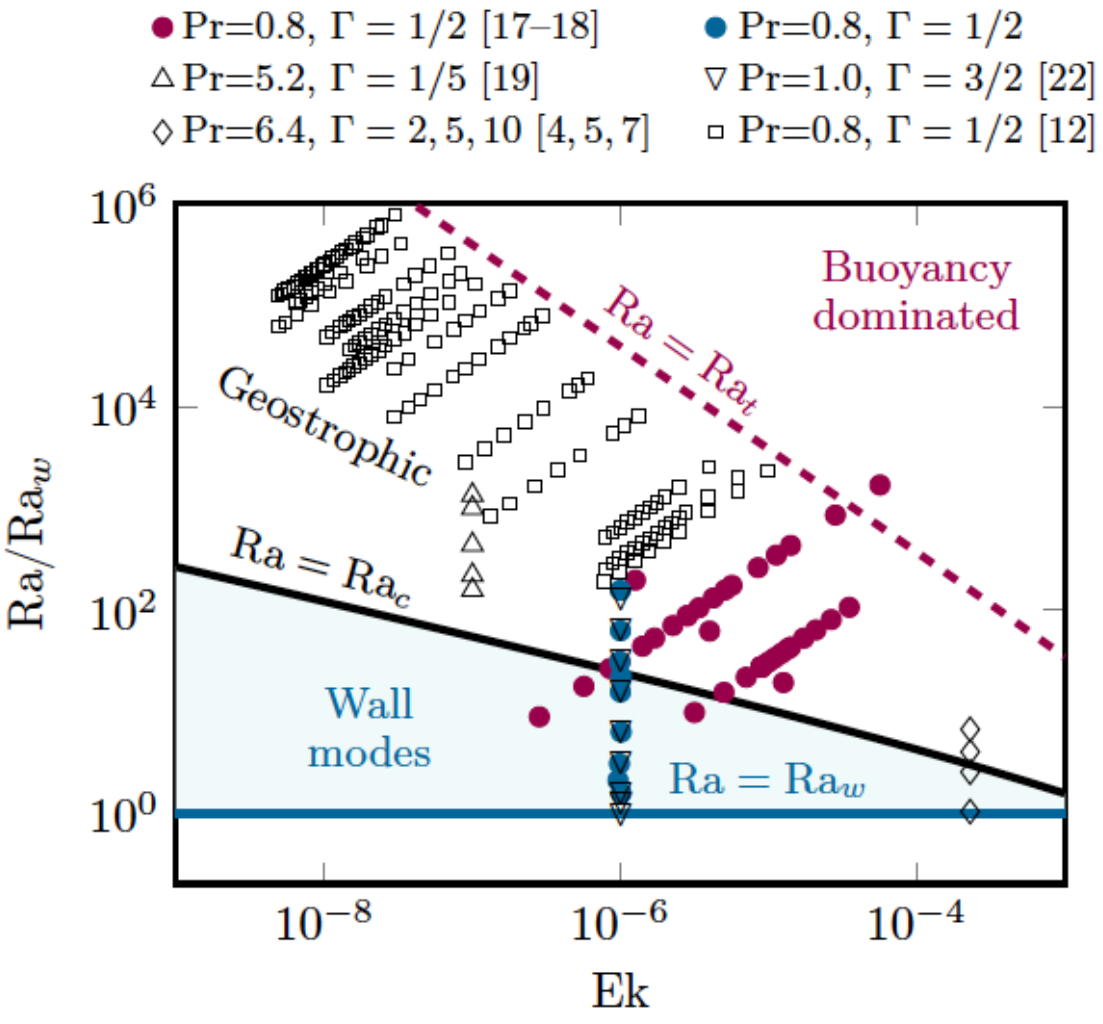

Ecke et al., PR Fluids **7**, L011501 (2022); cf. Goldstein et al., JFM **248**, 583 (1993) and Zhang et al., JFM **915**, A62 (2021)

Robust boundary flow: $E = 10^{-6}$, $\sigma = 1$, $\Gamma = 1.5$

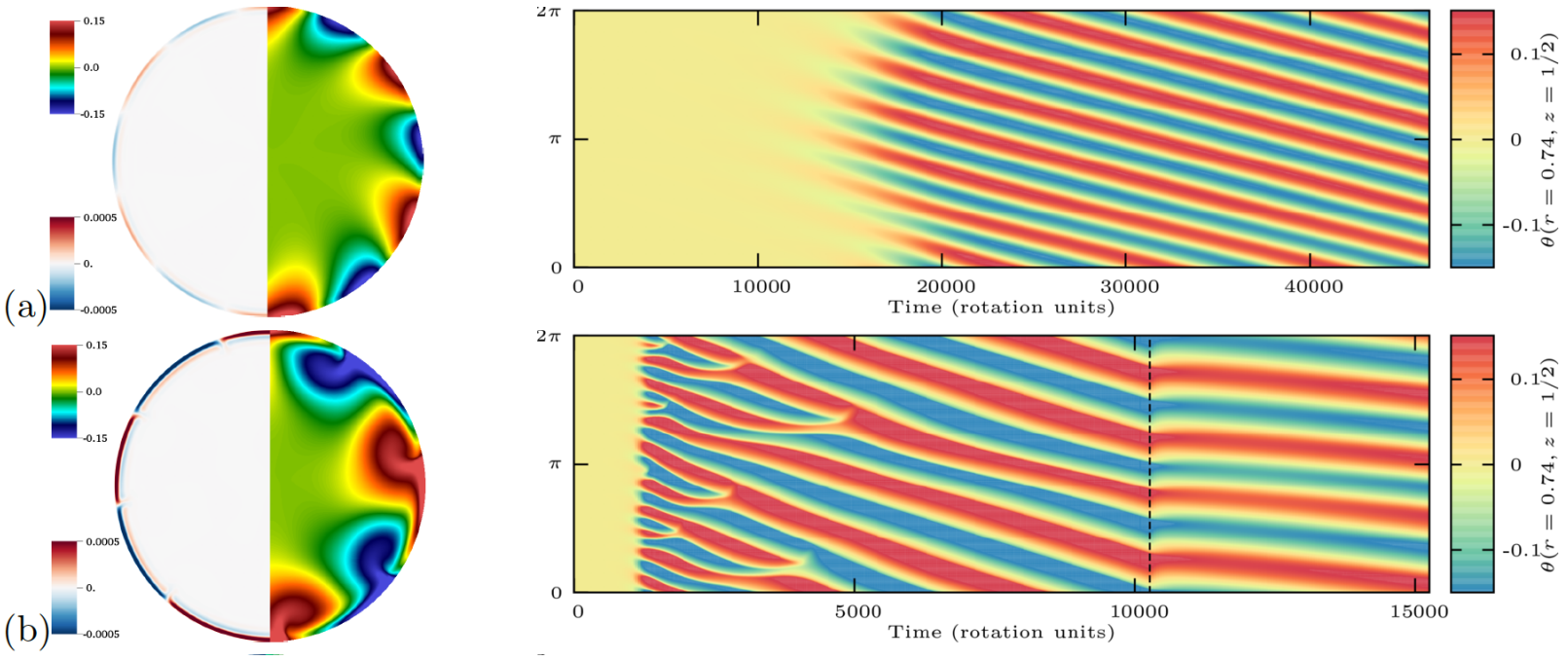

Midplane vertical velocity w (left) and fluctuating temperature θ at $r = 0.74$ (right) at (a) $Ra = 5 \times 10^7$ and (b) $Ra = 2 \times 10^8$. In (b) Ra is reduced to $Ra = 5 \times 10^7$ at the dashed line to demonstrate multistability.

Favier and Knobloch, JFM **895**, R1 (2020)

Robust boundary flow: $E = 10^{-6}$, $\sigma = 1$, $\Gamma = 1.5$

Wall states persist in the presence of a turbulent bulk state in the interior:

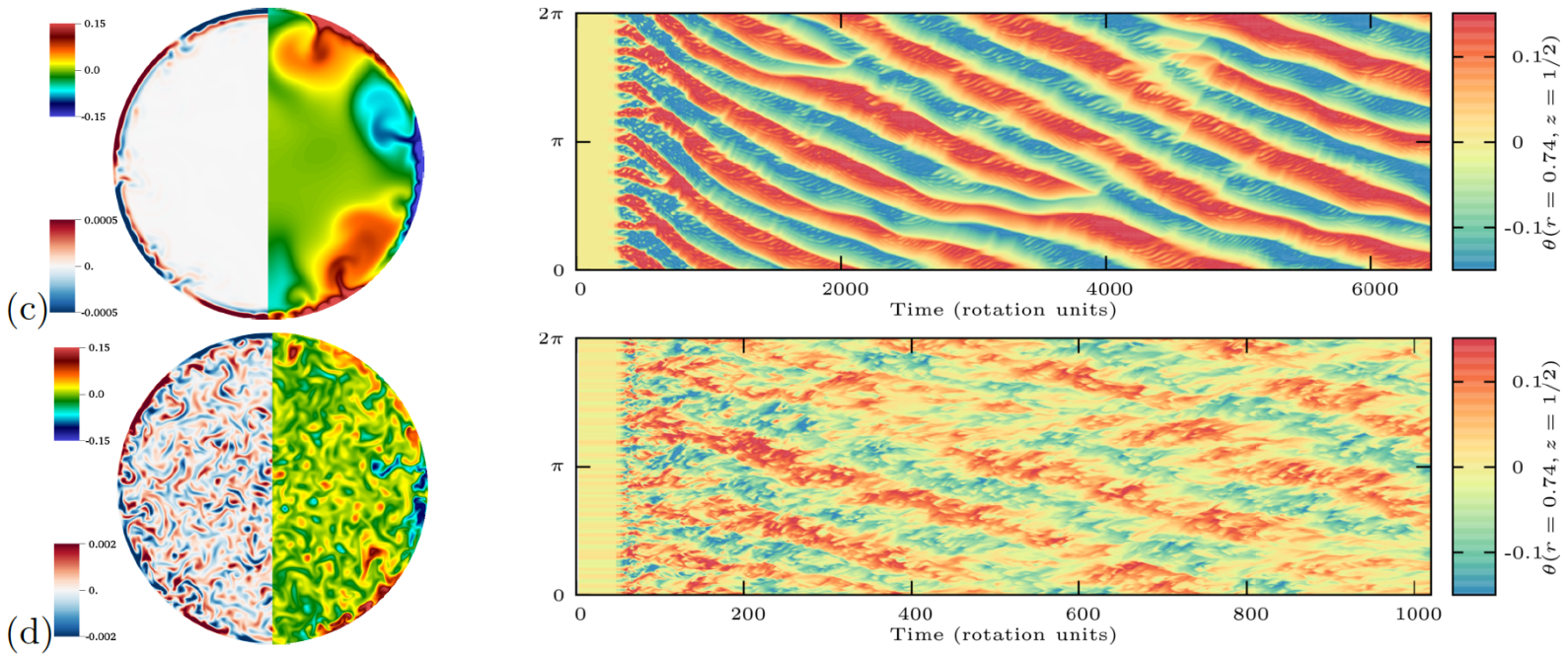

Midplane vertical velocity w (left) and fluctuating temperature θ (right) at (c) $Ra = 5 \times 10^8$ and (d) $Ra = 2 \times 10^9$.

Favier and Knobloch, JFM **895**, R1 (2020).

Robust boundary flow: $E = 10^{-6}$, $\sigma = 1$, $\Gamma = 1.5$

Wall states persist in the presence of a vertical barrier:

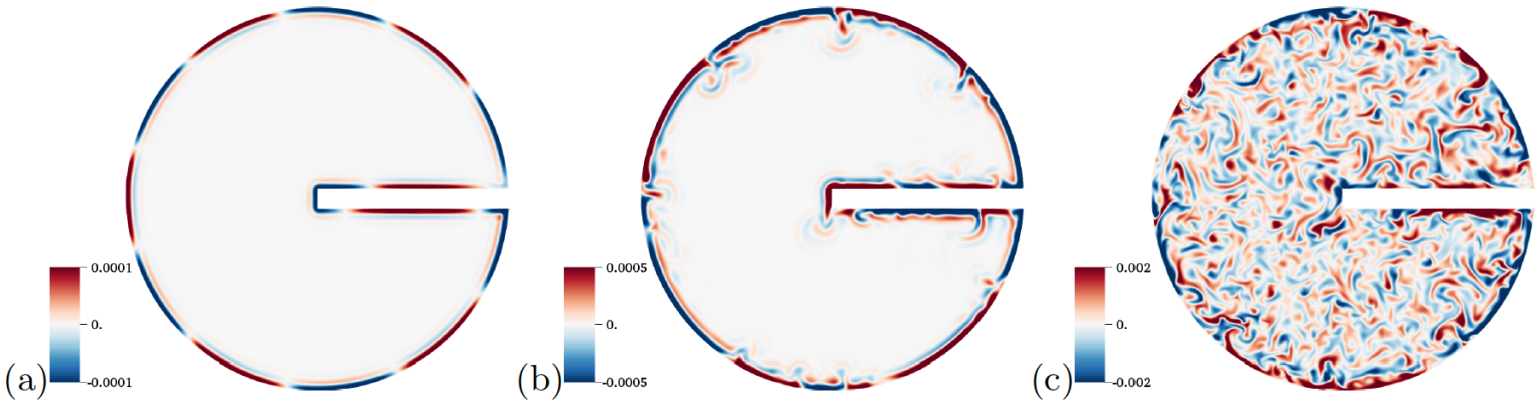

FIGURE 5. Vertical velocity in the mid-plane $z = 0.5$ for a cylinder with a barrier. The Rayleigh number increases from left to right: (a) $Ra = 5 \times 10^7$, (b) $Ra = 5 \times 10^8$ and (c) $Ra = 2 \times 10^9$. Parameters are $\Gamma = 1.5$, $E = 10^{-6}$ and $Pr = 1$.

Favier and Knobloch, JFM **895**, R1 (2020)

Sound waves in chiral systems with odd viscosity

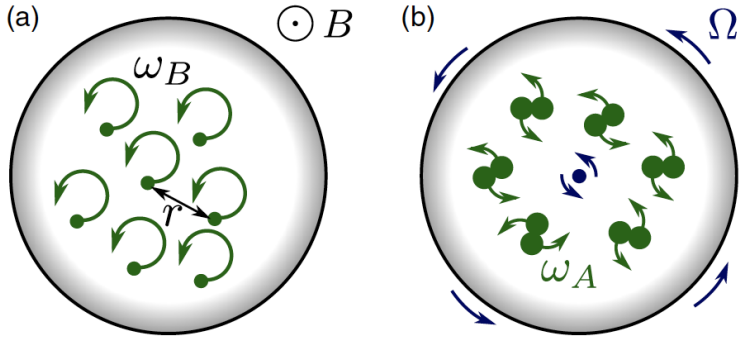

FIG. 1. Physical realizations of the minimal model for topological fluids with odd viscosity. (a) Two-dimensional plasma under magnetic field B, with cyclotron frequency $\omega_B = qB/M$. (b) Chiral active fluid with intrinsic rotation angular frequency ω_A, subject to a global rotation with angular frequency $\omega_B = -2\Omega$.

penetration depths vanish while the other half retain a finite penetration depth set by the gap size.

Model.—Consider the odd Navier-Stokes equations describing a compressible time-reversal and parity violating fluid,

$$\partial_t \rho(\mathbf{r}, t) = -\rho_0 \nabla \cdot \mathbf{v}(\mathbf{r}, t) \tag{1}$$

$$\partial_t \mathbf{v} = -c^2 \nabla \rho / \rho_0 + \omega_B \mathbf{v}^* + \nu^o \nabla^2 \mathbf{v}^*, \tag{2}$$

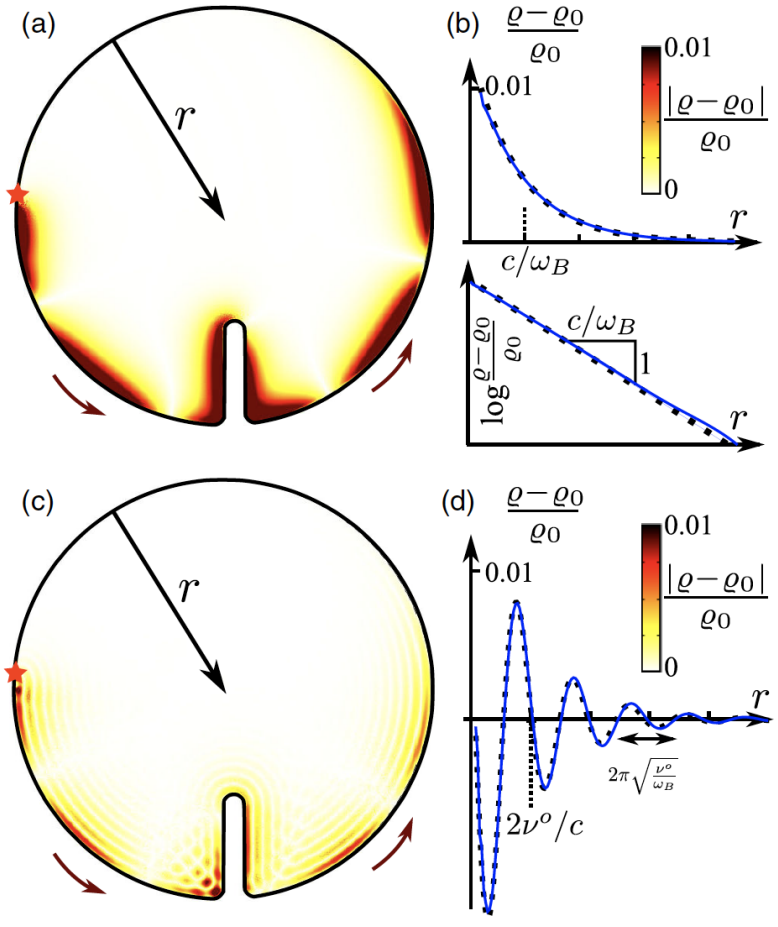

Souslov et al., PRL **122**, 128001 (2019)

Conclusions

We have exhibited a variety of localized standing and traveling states in two model systems: CSHE35 and the Purwins model. Both support wall and bulk states with similar properties. We constructed bifurcation diagrams for both cases. For this pde2path is an extremely helpful tool. In particular:

- LSW snake much like localized steady states in SHE
- LTW also exhibit snaking
- wall states on a disk closely resemble 1D states but with stronger forcing may interact with bulk states
- DNS starting from unstable states generate new states whose provenance remains unknown

H. Uecker, N. Verschueren and E. Knobloch, Localized dynamic patterns in the complex cubic-quintic Swift-Hohenberg equation in one and two dimensions, Chaos (2026)

E. Knobloch, S.O. Modai, H. Uecker and A. Yochelis, Localized spatiotemporal reaction-diffusion patterns on a line and a disk arising from a subcritical finite wavenumber Hopf instability, arXiv:2603.15161